Chapter 15
Methane Seeps in the Late Cretaceous Western Interior Seaway, USA

Neil H. Landman, J. Kirk Cochran, Jamie Brezina, Neal L. Larson, Matthew P. Garb, Kimberly C. Meehan, and Corinne Myers

15.1 Introduction

Hydrocarbon seep deposits, in one form or another, have been studied in the Upper Cretaceous Western Interior of North America since the end of the nineteenth century (Gilbert and Gulliver 1895). The broad geographic and stratigraphic distribution of these deposits suggests that they comprised one of the largest and most long-lived seep fields on the planet (Metz 2010). These seeps formed in the Western Interior Seaway (WIS) in relatively shallow water and attracted a wide variety of

N. H. Landman (✉)
Department of Invertebrate Paleontology, American Museum of Natural History, New York, NY, USA
e-mail: landman@amnh.org

J. K. Cochran
Department of Invertebrate Paleontology, American Museum of Natural History, New York, NY, USA

School of Marine and Atmospheric Sciences, Stony Brook University, Stony Brook, NY, USA

J. Brezina
Department of Mining Engineering, South Dakota School of Mines and Technology, Rapid City, SD, USA

N. L. Larson
Larson Paleontology Unlimited, Keystone, SD, USA

M. P. Garb
Department of Earth and Environmental Sciences, Brooklyn College, Brooklyn, NY, USA

K. C. Meehan
Department of Geology, University at Buffalo (SUNY, Buffalo), Buffalo, USA

C. Myers
Department of Earth and Planetary Sciences, University of New Mexico, Albuquerque, NM, USA

A. Kaim et al. (eds.), *Ancient Hydrocarbon Seeps*, Topics in Geobiology 53,
https://doi.org/10.1007/978-3-031-05623-9_15

organisms, including ammonites, inoceramids, gastropods, crabs, tube worms, echinoderms, and chemosymbiotic lucinids (Fig. 15.1). Most of the fauna comprised the same taxa as in the rest of the WIS, but it also included species that were unique to these sites.

The nature of these deposits has been debated since their discovery. Gilbert and Gulliver (1895) suggested, among other hypotheses, that these structures formed as the result of favorable conditions on the sea floor over long periods of time promoting the colonization of lucinid bivalves. Dane et al. (1937) speculated that the deposits formed as the result of precipitation due to submarine springs of low volume, but relatively high concentrations of calcium carbonate, producing hospitable sites for the growth of many kinds of organisms. Petta and Gerhard (1977) suggested that the deposits formed due to sediment baffling around grass beds in shallow marine lagoons, producing large mounds of carbonate mud. According to this hypothesis, the calcium carbonate in the deposits accumulated from the breakdown of calcareous chlorophytes and calcareous epibionts that were attached to the grasses. Not until the seminal studies of Kauffman et al. (1996), which utilized detailed isotopic, stratigraphic, and paleontologic data, did the methane seep origin of these deposits become apparent.

The specimens illustrated in this chapter are reposited in the Department of Invertebrate Paleontology at the American Museum of Natural History (AMNH), New York, New York. The sites in South Dakota, Wyoming, Montana, and Nebraska are referred to by AMNH locality numbers and study numbers (WPT) and are listed in Appendix Table 15.1.

15.2 Geologic Setting

During the Late Cretaceous, the Western Interior Foreland Basin was occupied by a broad seaway that extended from the proto-Gulf of Mexico to the western Canadian Arctic (Cobban and Reeside 1952; Gill and Cobban 1966; Kauffman and Caldwell 1993) (Fig. 15.2). The western shore of the WIS was bordered by a north-south trending unstable cordillera, and the eastern margin was formed by the low-lying stable platform of the eastern part of the conterminous USA and Canada (Cobban et al. 1994; Larson et al. 1997; Landman et al. 2010).

The geologic record of the Late Cretaceous WIS is rich in cephalopods and inoceramid bivalves, which has permitted a refined biostratigraphic zonation of this region. The ammonite zonation of the Upper Cretaceous Western Interior was first summarized by Cobban and Reeside (1952). Since then, it has undergone many revisions and presently consists of 66 zones, several of which are further subdivided into two, three, or four inoceramid zones. The presence of bentonites in the stratigraphic section has permitted determination of absolute ages based on $^{40}Ar/^{39}Ar$ analyses of the sanidines in the bentonites. We follow the standard biostratigraphic zonation of Cobban et al. (2006) in which the Campanian Stage is divided into three substages and the Maastrichtian Stage is divided into two substages (Fig. 15.2).

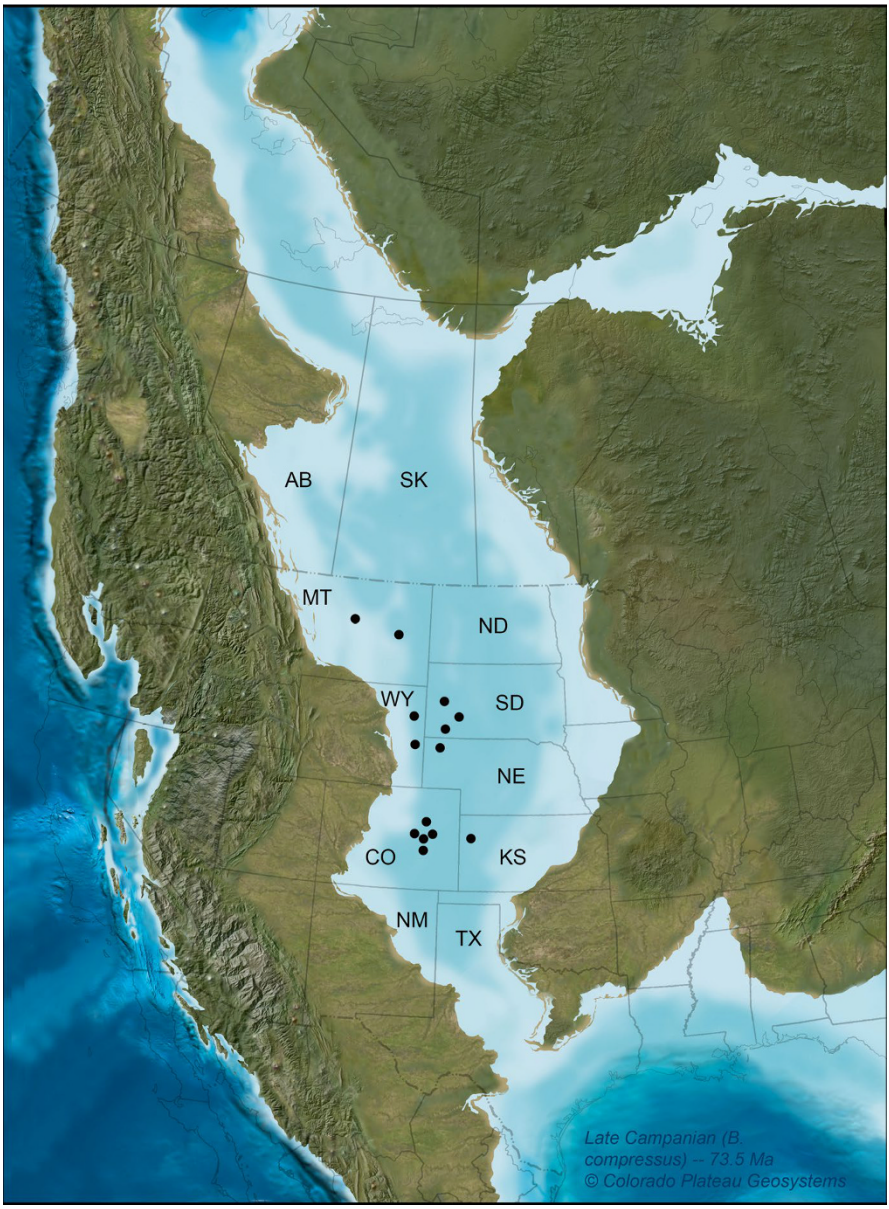

Fig. 15.1 Map of the Western Interior Seaway during the Late Cretaceous (late Campanian) showing main areas of methane seeps (dots) in Montana, Wyoming, South Dakota, Nebraska, Colorado, Utah, Kansas, and Texas (Blakey 2014, source map used with permission © 2021 Colorado Plateau Geosystems, Inc.). A single dot may represent multiple localities

SERIES	Stages	Substages	Ammonite zones	Inoceramid zones	Age (Ma)	Seeps
					66.0	
		Upper	*Hoploscaphites nebrascensis*			
			Hoploscaphites nicolleti			
			Hoploscaphites birkelundae			
	Maastrichtian	Lower	*Baculites clinolobatus*	*"Inoceramus" balchii*	69.59±0.36	
			Baculites grandis	*Trochoceramus radiosus*	70.00±0.45	*
			Baculites baculus	*"Inoceramus" incurvus*	71.96±0.08	
				Endocostea typica	71.98±0.31 72.50±0.31	*
UPPER CRETACEOUS (part)	Campanian	Upper	*Baculites eliasi*	*"Inoceramus" redbirdensis*		*
			Baculites jenseni	*"Inoceramus" oblongus*		*
			Baculites reesidei		73.41±0.46	*
			Baculites cuneatus	*"Inoceramus" altus*		*
			Baculites compressus		73.79±0.36	**
			Didymoceras cheyennense		74.67±0.15	**
			Exiteloceras jenneyi	*Sphaeroceramus pertenuiformis*	75.08±0.11	*
			Didymoceras stevensoni		75.16±0.12	*
			Didymoceras nebrascense	*"Inoceramus" tenuilineatus*	75.19±0.28	***
		Middle	*Baculites scotti*		75.56±0.11 75.84±0.26	***
			Baculites reduncus			
			Baculites gregoryensis			*
			Baculites perplexus	*Cataceramus subcompressus*		*
			Baculites sp. (smooth)			
			Baculites asperiformis			
			Baculites maclearni	*"Inoceramus" azerbaydjanensis*		
			Baculites obtusus		80.58±0.55	
		Lower	*Baculites* sp. (weak flank ribs)			
			Baculites sp. (smooth)	*Cataceramus balticus*		
			Scaphites hippocrepis III			
			Scaphites hippocrepis II		81.86±0.36	
			Scaphites hippocrepis I			
			Scaphites leei III	*Sphenoceramus lundbreckensis*	83.6±0.2	

Fig. 15.2 Biostratigraphic zonation of the Upper Cretaceous Western Interior (Cobban et al. 2006) showing intervals with methane seep deposits (asterisks). The number of asterisks indicates the relative abundance of seep deposits. Absolute ages are updated from Lynds and Slattery (2017) and Landman et al. (2018a, b)

During the Late Cretaceous, the WIS formed an episodically restricted, shallow epicontinental sea. The climate was warm during a "greenhouse" interval of Earth history, with little to no permanent polar ice and a latitudinal temperature gradient reduced by up to 50%, as compared with today (Barron 1983; Covey et al. 1996; Huber et al. 2002; Spicer and Corfield 1992; Jenkyns et al. 2004; Hay 2008). Eustatic as well as regional sea level oscillations significantly impacted water chemistry and mixing during the approximately 35 Myr in which the WIS was "open" to both the proto-Gulf of Mexico and Arctic Oceans. This has made detailed oceanography of the WIS challenging to reconstruct, but some aspects are clear. The WIS was generally shallow ($\leq$100 m), with substantial input of freshwater from surface runoff and groundwater leaching from the cordillera (Kauffman 1984; Fricke et al. 2010; Cochran et al. 2003). Mixing of warmer, saltier waters from the south with colder, fresher waters from the north may have led to some degree of periodic water stratification and even at times a brackish water cap (Wright 1987; Corbett and Watkins 2013; Fisher and Arthur 2002; Schröder-Adams 2014; He et al. 2005). Periods of higher sea level (e.g., middle Campanian) likely reflected more "normal marine" environments in the WIS with better vertical mixing and an oxygenated bottom. In contrast, during periods of lower sea level (e.g., late Campanian-Maastrichtian), the WIS experienced significant restriction to open ocean circulation (especially to the north), and bottom waters became substantially less oxygenated (Kauffman 1984; Tsujita and Westermann 1998; Fisher and Arthur 2002; Schröder-Adams 2014).

15.3 Geomorphology of Seep Deposits

Seep deposits in the Upper Cretaceous Western Interior in the area around Pueblo, Boone, and Colorado Springs, Colorado, were called "tepee buttes" by Gilbert and Gulliver (1895) (Fig. 15.3a). They were so called because of their superficial resemblance to the tepees or lodges of the Shoshone and other American Plains Indians. These stony outcroppings are conical in shape and up to 20 m in height with circular bases up to 60 m in diameter and flat to pointed summits 3–8 m in diameter (Fenneman 1931). The top of each butte is held up by fossiliferous limestone blocks, which often tumble down the slopes, creating a layer of colluvium that protects the slopes from erosion. In classic tepee buttes, the surrounding soft shale has partially eroded away leaving the hard, resistant limestone projecting at the top, with soft sedimentary deformation features occasionally appearing underneath the limestone.

Seep deposits elsewhere in the Upper Cretaceous Western Interior can assume many other forms, however, depending on the size, shape, and lithology of the carbonates that make up the deposits (Figs. 15.3, 15.4 and 15.5). The abundance and distribution of fossils are also important factors in determining how the deposits appear. In some instances, for example, massive accumulations of indurated lucinids produce hard, resistant blocks that cover the surface of the deposits, making them resistant to erosion (Fig. 15.5b). The appearance of the deposits ultimately depends on how much weathering has taken place and how much of the surrounding

Fig. 15.3 Close-ups of methane seep deposits in the Pierre Shale of Colorado, Wyoming, South Dakota, and Nebraska. (**a**) Classic "tepee butte" along the Front Range of Colorado, as illustrated by Gilbert (1896: pl. 67). (**b**) Overview of seep deposits at AMNH loc. 3494, *Baculites scotti-Didymoceras nebrascense* Zones, Pierre Shale, Weston County, Wyoming. Photo by S. Klofak. (**c**) Overview of seep deposit at AMNH loc. 3812, Pierre Shale, Custer County, South Dakota. The seep deposit forms a long ridge approximately 100 m in length with a lower mound at one end and a higher mound on the other end, so that the total difference in height is approximately 10 m. The fossils at the bottom belong to the *D. cheyennense* Zone, and the fossils at the top belong to the *B. compressus* Zone. (**d**) Close-up of seep deposit at AMNH loc. 3344, *B. scotti-D. nebrascense* Zones, Pierre Shale, Butte County, South Dakota. Photo by B. Brown. E. Seep deposit near AMNH loc. 3344, *B. scotti-D. nebrascense* Zones, Pierre Shale, Butte County, South Dakota. Photo by B. Brown. (**f**) Overview of seep deposits, AMNH loc. 3666, *B. scotti-D. nebrascense* Zones, Pierre Shale, Sioux County, Nebraska. These are among some of the largest fossil seep deposits on the planet

Fig. 15.4 Methane seep deposits in the Pierre Shale, South Dakota. Photos by S.M. Klofak and M.P. Garb. (**a**) Exposure of seep deposit in cross section revealing the main carbonate body (arrow), AMNH loc. 3528, *Baculites compressus* Zone, Pierre Shale, Meade County, South Dakota. (**b**) Exposure of seep deposit in cross section, AMNH loc. 3504, *B. compressus* Zone, Pierre Shale, Custer County, South Dakota. The main carbonate body (arrow) is approximately 2.5 m wide. (**c**) Exposure of seep deposit in cross section, AMNH 3418, *Didymoceras cheyennense* Zone, Pierre Shale, Custer County, South Dakota. (**d**) Close-up of pipes (arrow) at AMNH loc. 3418, *D. cheyennense* Zone, Pierre Shale, Custer County, South Dakota. E. Specimen of *Placenticeras* sp. embedded in shale at AMNH loc. 3528, *B. compressus-B. cuneatus* Zones, Pierre Shale, Meade County, South Dakota. (**f**) Close-up of pipes and subspherical SACs at AMNH loc. 3528, *B. compressus* Zone, Pierre Shale, Meade County, South Dakota

host rock still remains. It is important to emphasize that the shape of the deposits in the present-day landscape may bear little resemblance to their shape as topographic features on the ancient sea floor.

Seep deposits in the Upper Cretaceous Western Interior also appear as steep chimneys or pinnacles informally known as “rock haystacks” 5–10 m in height and

Fig. 15.5 Methane seep deposits in the Pierre Shale, South Dakota. Photos by M.P. Garb. (**a**) Exposure of seep deposit in cross section, AMNH loc. 3440, *Didymoceras nebrascense* Zone, Pierre Shale, Butte County, South Dakota. (**b**) Close-up of specimens of *Nymphalucina occidentalis*, AMNH loc. 3440, *D. nebrascense* Zone, Pierre Shale, Butte County, South Dakota. (**c**) Seep deposit, AMNH loc. 3529, *D. cheyennense* Zone, Pierre Shale, Pennington County, South Dakota. (**d**) Seep deposit, AMNH loc. 3419, *Baculites compressus* Zone, Pierre Shale, Custer County, South Dakota. (**e**) Micritic mass, AMNH loc. 3545, *B. compressus-B. cuneatus* Zones, Pierre Shale, Meade County, South Dakota. (**f**) Close-up of micritic mass with burrow markings, AMNH loc. 3545, *B. compressus-B. cuneatus* Zones, Pierre Shale, Meade County, South Dakota

2–3 m in diameter with all of the surrounding shale eroded away, as exposed in the area around Newell, Butte County, South Dakota (Fig. 15.3f). Seep deposits can form large grass-covered mounds informally known as "ant hills" as much as 20 m in height with circular bases 10–20 m in diameter, for example, in Weston County, Wyoming (Fig. 15.3b). Like tepee buttes, the ant hills are capped by limestone blocks, but the sides of the deposits are more gently inclined. Occasionally, multiple ant hills coalesce together forming elongate ridges several 100 m in length, with a series of small peaks along the tops of the ridges, for example, in Sioux County, Nebraska, which may represent some of the largest seep deposits on the planet (Fig. 15.3f).

Seep deposits can also appear as low-lying, hard limestone mounds free of grass cover, roughly elliptical in outline with dimensions of 30 m × 15 m and as much as 5 m high, bearing an uncanny resemblance to Paleozoic reefs, as in the deposits in the Ojinaga Formation, Texas, and those in the Pierre Shale in Custer County, South Dakota (Fig. 15.5c, d). They can also appear as small broken-up masses of carbonate rubble with dimensions of 2 m × 2 m and 0.5 m high, which can usually be spotted from a distance by a break in the vegetation (Fig. 15.3d). Indeed, changes in the vegetation are a clue to the existence of a seep deposit because of the presence of the carbonates themselves and iron and sulfur minerals in the shale. Finally, the deposits can appear in cross section in stream and river cuts (Fig. 15.4a–c). In these exposures, the light-gray-weathering, massive carbonate bodies stand out in sharp contrast to the surrounding gray- to black-weathering shales (Fig. 15.5e, f).

15.4 Geographic Distribution

Methane seep deposits are geographically widespread throughout the Upper Cretaceous Western Interior (Fig. 15.6). From west to east, they stretch from south-central Colorado along the Front Range of the Rockies (Kauffman et al. 1996) to western Kansas (Elias 1933). They occur as far south as Presidio County, West Texas (Metz 2002), and southern Utah (Kiel et al. 2012). In the area around the Black Hills, they occur in northeastern Wyoming (Landman et al. 2013), northwestern South Dakota (Landman et al. 2013), southwestern South Dakota (Larson et al. 2014; Cochran et al. 2015; Hunter et al. 2016), and northwestern Nebraska. In Montana, they are present on the Miles City Arch in Carter County, on the Porcupine Dome in Garfield and Rosebud counties, on the Cedar Creek Anticline in Dawson County (Landman et al. 2020; Ryan et al. 2020), in the Cat Creek and Devils Basin oilfields in Petroleum and Musselshell counties, and in the Fort Peck area in McCone and Valley counties. They occur as far north as Alberta, Canada (Collom and Johnston 2000). Based on the distribution of seep deposits in Colorado, South Dakota, Montana, Wyoming, and Kansas, Landman et al. (2012) estimated that they cover an area of 13,350 km^2. However, this figure is undoubtedly an underestimate, as it is biased by the limited availability of outcrops. In fact, pieces of seep carbonates are occasionally found on gravel bars along the streams and rivers draining the

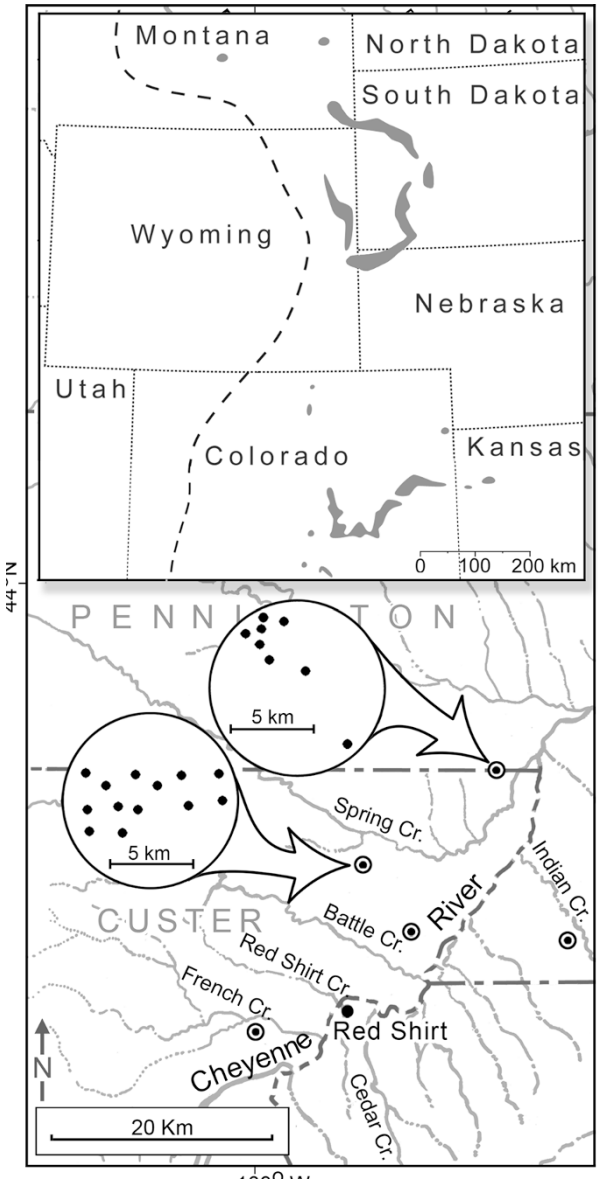

Fig. 15.6 Overview: Distribution of seep deposits in the Upper Cretaceous Western Interior Seaway (shaded locations of seeps in the top panel from Metz (2010)). The dashed line represents the western shoreline of the WIS during the deposition of the *Didymoceras cheyennense* Zone. Close-up: Distribution of methane seeps in the *D. cheyennense* and *Baculites compressus* Zones of the Pierre Shale in southwestern South Dakota

Black Hills, especially in western South Dakota, suggesting the existence of additional seep deposits, now eroded away.

The distribution of seep deposits has been mapped in minute detail in certain areas. In the region around the Black Hills in South Dakota and Wyoming, seep deposits have been mapped by Darton (1902, 1904, 1905, 1919), Darton and O'Hara (1909), Darton and Paige (1925), and Mapel and Pillmore (1963); in Colorado, they have been mapped by Fisher (1906), Finlay (1916), Lavington (1933), and Sharps (1976, 1980); and in Kansas by Elias (1931). These maps reveal the ubiquity of the deposits. For example, in 1 mi^2 section just east of Oelrichs, Fall River County, South Dakota, Darton (1902) mapped 45 seep deposits (Fig. 15.7). In 1 mi^2 section north of Newell, Butte County, South Dakota, Darton (1919) mapped 65 deposits (Fig. 15.8). Altogether, Metz (2010) counted 1350 seep deposits based on an examination of the geologic maps of Colorado and South Dakota prepared by the US Geological Survey between 1895 and 1936.

In addition to their abundance, two other patterns emerge in examining the geographic distribution of these deposits. First, they usually occur in clusters. For example, in the map by Darton (1919) of Fall River County, South Dakota, as many as six deposits occur in tight clusters (Fig. 15.7). Second, the seep deposits usually occur in linear arrangements. For example, in the map cited above, as many as 12 deposits occur in a straight line over a distance of approximately 1 km. These patterns may reflect the original distribution of seeps on the sea floor. They may further reflect fault lines that existed in the basin during the Late Cretaceous and facilitated upward fluxes of methane toward the sediment-water interface. Indeed, Gilbert (1897) noted that seep deposits in the area near Pueblo, Colorado, are oriented in a north-south belt paralleling the Rocky Mountains Front, possibly reflecting faults associated with the Laramide orogeny (Metz 2010). Larson et al. (2014) also suggested that seeps around the Black Hills formed from fluids and gasses migrating along faults and fractures in the Late Cretaceous prior to the uplift of the Black Hills (see below).

It is important to emphasize, however, that the present-day distribution of seep deposits is limited by the available outcrop. The availability of outcrop depends on such features as anticlines that bring rocks of the appropriate age to the surface. It also depends on the pattern of streams and rivers that erode the landscape to expose these rocks. Therefore, the abundance of seep deposits today is an underestimate of the original number of seeps on the sea floor. It is likely that they formed extensive seep fields covering broad stretches of the basin.

15.5 Stratigraphic Distribution

Methane seep deposits formed in the Western Interior of North America from the late Cenomanian to the early Maastrichtian (Fig. 15.2). The oldest methane seep deposits occur in the upper Cenomanian *Metoicoceras geslinianum* and *Neocardioceras juddi* Zones in the Tropic Shale of Utah (Kiel et al. 2012). The next younger deposits occur in the upper Coniacian *Scaphites* (*S.*) *depressus* Zone in the

Fig. 15.7 Map of tepee buttes near Newell, Butte County, South Dakota (Darton 1919). The dots represent seep deposits

oolitic limestones of the Bad Heart Formation of Alberta (Collom and Johnston 2000). The next younger deposits occur in the lower Campanian *Submortoniceras tequequitense* Zone in the upper Ojinaga Formation of the Sierra Vieja region, Presidio County, West Texas (Metz, 2002).

The rest of the seep deposits in the Upper Cretaceous Western Interior occur in the Pierre Shale in Colorado, Kansas, Wyoming, South Dakota, Nebraska, and

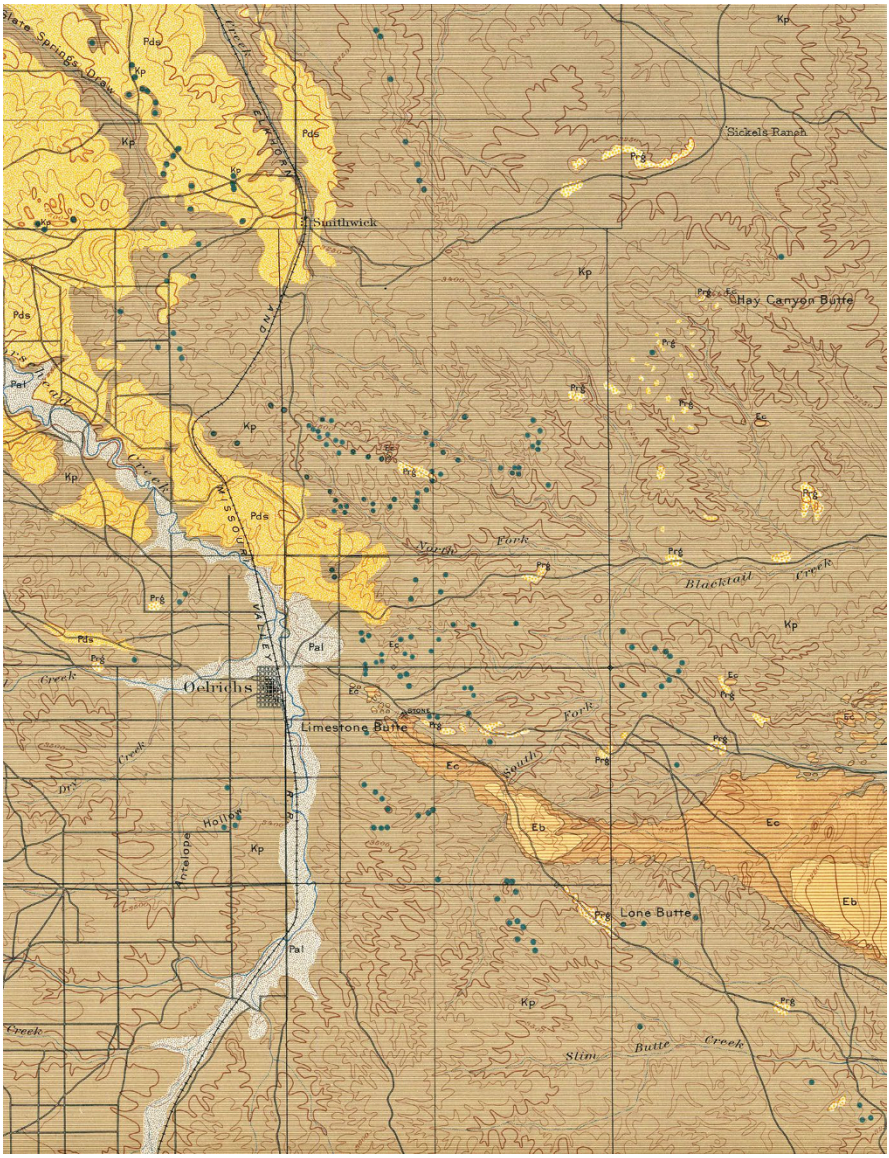

Fig. 15.8 Map of tepee buttes near Oelrichs, Custer County, South Dakota (Darton 1902). The dots represent seep deposits

Montana and the Bearpaw Shale in Montana and Canada (time equivalent to the upper Pierre Shale). The Pierre Shale is approximately 1000 m thick at its informal reference section at Red Bird, Wyoming, and consists of organic-rich dark- to light-gray-weathering clayey to silty shale (Gill and Cobban 1966). The seep deposits in the Pierre Shale extend from the middle Campanian to the lower Maastrichtian,

spanning 6–7 Myr (Fig. 15.2). However, the abundance and geographic extent of the seep deposits in the Pierre Shale vary throughout this time interval.

The oldest seep deposits in the Pierre Shale occur in the middle Campanian *Baculites perplexus* and *B. gregoryensis*Zones, but these deposits have only been reported from two sites. Gill and Cobban (1966) reported tepee butte deposits of this age from the upper part of the Mitten Shale Member and lower part of the Red Bird Silty Member of the Pierre Shale in Niobrara County, east-central Wyoming. Scott and Cobban (1986b) reported tepee butte deposits from the *B. gregoryensis* Zone in the uppermost beds of the Mitten Shale Member near Round Butte, Colorado.

The most widespread and abundant seep deposits in the Pierre Shale occur in the upper middle Campanian *Baculites scotti* and lower upper Campanian *Didymoceras nebrascense* Zones. These are the deposits that were originally described as tepee buttes from Colorado (Fig. 15.3a) by Gilbert and Gulliver (1895). They occupy what is called "the tepee butte zone" of the Pierre Shale near Fountain, Pueblo, and Boone in east-central Colorado (Gilbert 1897; Lavington 1933; Scott 1969; Scott and Cobban 1986a; Kauffman et al. 1996, Bishop and Williams 2000). These deposits are also present in other areas of Colorado including the Cañon City-Florence area, north of Walsenburg, west of Gardner at Huerfano Park (Scott and Cobban 1975; Howe and Kauffman 1986), west of Colorado Springs between Hugo and Kit Carson (Lavington 1933), west of Berthoud (Lavington 1933; Scott and Cobban 1965), and near Round Butte (Scott and Cobban 1986b).

Seep deposits of this age are also common in parts of South Dakota, Wyoming, and Nebraska. They are present in Weston and Crook counties in northeastern Wyoming (Landman et al. 2013); Butte County in northwestern South Dakota (Darton 1919; Bishop and Williams 2000; Landman et al. 2013); Pennington, Meade, Custer, and Fall River counties in southwestern South Dakota (Darton 1902; Bishop and Williams 2000; Landman et al. 2012; Larson et al. 2014; Hunter et al. 2016; Kato et al. 2017); and Sioux County in northwestern Nebraska. Seep deposits have also been identified from the two overlying zones (*Didymoceras stevensoni* and *Exiteloceras jennyi* Zones) in Carter County, Montana.

The second most widespread and abundant seep deposits in the Pierre Shale occur in the upper Campanian *Didymoceras cheyennense*, *Baculites compressus*, and *B. cuneatus* Zones. These deposits are locally common in Meade, Pennington, and Custer counties, southwestern South Dakota (Darton 1902, 1919; Landman et al. 2012, 2018a, b; Larson et al. 2014; Hunter et al. 2016; Kato et al. 2017). Elias (1933) also reported seep deposits of this age in the upper part of the Weskan Shale Member of the Pierre Shale in Wallace County, western Kansas.

In the upper part of the upper Campanian, seep deposits are present, but they have not yet been well documented. They occur in the *B. reesidei* and possibly *B. jenseni* Zones in the Bearpaw Shale on the Porcupine Dome and Cat Creek Anticline, Montana, and in the *B. reesidei-B. eliasi* Zones in the Salt Grass Member of the Pierre Shale in Wallace County, western Kansas (Elias 1933). They also occur in the *B. eliasi* Zone in the upper part of the Pierre Shale southwest of Longmont, Colorado (Scott and Cobban 1965), and in the same zone in the Kara Bentonitic

Member and overlying part of the Pierre Shale in Crook and Weston Counties, Wyoming (Robinson et al. 1959, 1964).

In the lower Maastrichtian, seep deposits occur in the *Baculites baculus* Zone in the lower part of the upper unnamed shale member of the Pierre Shale in Niobrara County, Wyoming (Gill and Cobban 1966). They occur at the base of this zone in the Pierre Shale on the Cedar Creek Anticline in Dawson County, Montana (Landman et al. 2019, 2020; Ryan et al. 2020). Finally, seep deposits have been reported from the *B. grandis* and *B. clinolobatus* Zones in the Beecher Island Shale Member of the Pierre Shale in Wallace County, western Kansas (Elias 1933).

15.6 Methods of Study

The seep deposits in the Upper Cretaceous US Western Interior have been extensively studied over the last 25 years. Over the course of these studies, samples of limestone and well-preserved shell material have been analyzed for carbon, oxygen, and strontium isotopes (Kauffman et al. 1996; Krauss et al. 2009; Landman et al. 2012, 2018a, b; Cochran et al. 2015). Shell material has been screened to determine the quality of preservation according to the *Preservation Index (PI)* published by Cochran et al. (2010), utilizing only material with PI $\geq$3 for isotopic analyses. The mineralogy of the limestones has been studied in bulk and thin section using scanning electron microscopy (SEM), X-ray diffraction analysis (XRD), and electron microprobe (EMP). The limestone has also been analyzed for biomarkers to detect the former presence of sulfate-reducing bacteria (Birgel et al. 2006).

The structural framework and faunal composition of the seep deposits have been examined in detail. The seep deposits from the *Baculites scotti-Didymoceras nebrascense* Zones of the Pierre Shale of Colorado have been investigated by Howe (1987) and Kauffman et al. (1996) by taking blocks of limestone along the long and short axes of deposits as well as from the surrounding shale. The blocks were 30 cm × 30 cm and were extracted at 1 m intervals, labeled, and brought back to the laboratory for polishing and dissection. In contrast, the seep deposits from the *B. scotti-B. baculus* Zones of the Pierre Shale of South Dakota, Wyoming, Nebraska, and Montana, were sampled by intensive surface collecting and breaking off fresh chunks of limestone. Wherever feasible, fossils were collected in situ. However, it is always possible to confound variation in spatial distribution with variation in stratigraphic distribution due to downward slide of material. Samples were brought back to the laboratory for identification, preparation, and isotopic analysis (Landman et al. 2012; Meehan and Landman 2016; Hunter et al. 2016; Rowe et al. 2020; Ryan et al. 2020).

Some seep deposits were fortuitously exposed in cross section along stream and river cuts allowing for a detailed analysis of the seep structure and faunal distribution. Fossils and seep-associated concretions (SACs) were mapped with respect to their distance from the main carbonate body. At AMNH loc. 3418 from the *Didymoceras cheyennense* Zone of the Pierre Shale, Custer County, South Dakota,

the face of the exposure was mapped using a grid work of ropes attached to the outcrop to subdivide the deposit into 1 m^2 sections, allowing us to record the location of fossils and SACs (Fig. 15.4c, d). In these instances, it was theoretically possible to tease out spatial from stratigraphic variation, but even here, it is not always easy to trace the same event bed throughout the stratigraphic section.

15.7 Oxygen and Carbon Isotopic Composition

The oxygen and carbon isotopic composition of seep carbonates and associated shells of well-preserved fossils provides important clues about the seep environment. Values of $\delta^{13}C$ of seep carbonates are commonly much lower than those in age-equivalent non-seep deposits elsewhere in the basin (Fig. 15.9). For example, in seep deposits from the upper Cenomanian *Metoicoceras geslinianum* and *Neocardioceras juddi* Zones in the Tropic Shale of Utah, the values of $\delta^{13}C$ range from −25‰ to −21‰ at one site and −37‰ to −33‰ at another site (Kiel et al. 2012). In seep deposits from the lower Campanian *Submortoniceras tequequitense* Zone in the upper Ojinaga Formation of the Sierra Vieja region, Presidio County, West Texas, the values of $\delta^{13}C$ range from −35‰ to −26‰ at one site and −36‰ to −28‰ at another site (Metz 2002). In seep deposits from the middle Campanian *Baculites scotti*-upper Campanian *Didymoceras nebrascense* Zones of the Pierre Shale in Colorado, the values of $\delta^{13}C$ range from −45‰ to −40‰ (Kauffman et al. 1996). In seep deposits from the upper Campanian *D. cheyennense* Zone of the Pierre Shale in South Dakota, the values of $\delta^{13}C$ range from −47‰ to −12‰ (Landman et al. 2012). In seep deposits from the upper Campanian *B. compressus-B. cuneatus* Zones of the Pierre Shale in South Dakota, the values of $\delta^{13}C$ range from −51‰ to −37‰ (Landman et al. 2018). Finally, in seep deposits from the lower Maastrichtian *B. baculus* Zone of the Pierre Shale in Montana, the values of $\delta^{13}C$ range from −51.5‰ to −49.5‰ (Ryan et al. 2020).

In comparison, the values of $\delta^{13}C$ of concretionary matrix ($CaCO_3$) at age-equivalent non-seep sites are higher. For example, in the concretionary matrix at non-seep sites in the upper Campanian *Baculites compressus-B. cuneatus* Zones of the Pierre Shale in South Dakota, the value of $\delta^{13}C$ equals −22‰ (Landman and Klofak 2012). In the concretionary matrix at non-seep sites in the lower Maastrichtian *B. baculus* Zone of the Pierre Shale in Montana, the values of $\delta^{13}C$ range from −13‰ to −10‰ (Landman et al. 2015). The lower values of $\delta^{13}C$ of the carbonates in seep deposits compared with those in age-equivalent non-seep deposits are the result of the influence of anaerobic oxidation of methane (AOM) on the isotopic composition of the dissolved inorganic carbon (DIC) reservoir from which the seep carbonates precipitated (Boetius et al. 2000) (Fig. 15.9). (See Cochran et al. this volume, for further discussion of seep geochemistry; see the section on Faunal Composition for a comparison between the carbon isotopic compositions of well-preserved shell material at seep and age-equivalent non-seep sites.)

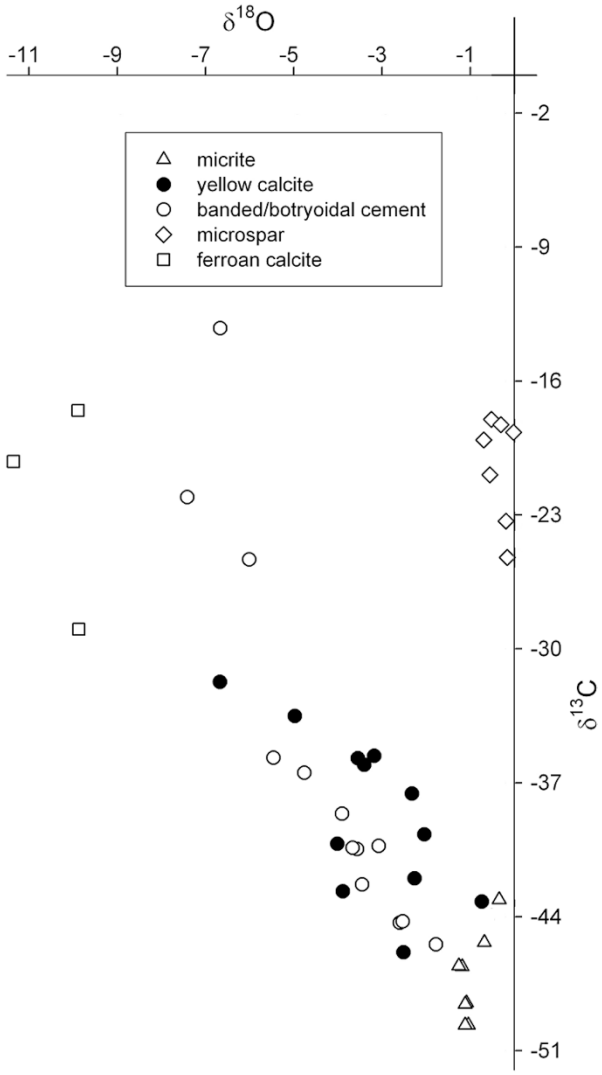

Fig. 15.9 Values of $\delta^{13}C$ and $\delta^{18}O$ of the seep carbonates from the *Baculites scotti-Didymoceras nebrascense* Zones of the Pierre Shale of Colorado (data replotted from Krause et al. (2009)). The low values of $\delta^{13}C$ of the seep carbonates (triangles) are due to the anaerobic oxidation of methane

In contrast, the values of $\delta^{18}O$ of the carbonates and well-preserved shell material (e.g., *Baculites*) at seep sites are similar to those of carbonates and well-preserved shell material at age-equivalent non-seep sites in other parts of the basin. For example, in seep carbonates from the upper Campanian *B. compressus-B. cuneatus* Zones of the Pierre Shale in South Dakota, the values of $\delta^{18}O$ range from −1‰ to 0‰ (Landman et al. 2018a, b). Similarly, in samples of well-preserved shell material

from the same site, the average values of $\delta^{18}O$ range from −2.5‰ to −0.3‰. In comparison, the value of $\delta^{18}O$ in the concretionary matrix from non-seep sites from the same time interval equals −2‰ (Landman and Klofak 2012). As well, in samples of well-preserved shell material from the same non-seep site, the average values of $\delta^{18}O$ range from −2‰ to −1‰ (Cochran et al. 2010).

The values of $\delta^{18}O$ in the carbonates and well-preserved molluscan shell material at seep sites translate into water temperatures of 15–25 ° C, using the equation of Grossman and Ku (1986) modified by Hudson and Anderson (1989) and assuming a value of −1‰ for the oxygen isotopic composition of the WIS (Shackleton and Kennett 1975; Dennis et al. 2013). This temperature range overlaps with that derived from analysis of carbonates and well-preserved shell material (e.g., *Baculites*) at age-equivalent non-seep sites elsewhere in the basin (e.g., He et al. (2005), Landman and Klofak (2012), Landman et al. (2015, 2018a, b). This similarity implies that the seep deposits were not hydrothermally driven but formed at the same temperature as the ambient water and thus are "cold" seeps (for more on modern cold seeps, see Kiel (2010)).

The isotopic values of the late burial cements in seep deposits exhibit a trend toward lower values of $\delta^{18}O$ and higher values of $\delta^{13}C$ (Kauffman et al. 1996). Krause et al. (2009) performed a series of analyses on the micritic limestone, ferroan calcite, yellow calcite, and botryoidal cement in seep deposits from the middle Campanian *Baculites scotti* and upper Campanian *Didymoceras nebrascense* Zones of the Pierre Shale in Colorado (Fig. 15.9). The values of $\delta^{13}C$ in the micritic limestone range from −50‰ to −43‰, and the values of $\delta^{18}O$ range from −1‰ to 0‰. On the other end of the spectrum, the values of $\delta^{13}C$ of the ferroan calcite range from −29‰ to −18‰, and the values of $\delta^{18}O$ range from −11‰ to −10‰. These trends indicate a series of late-stage diagenetic alterations, likely influenced by meteoric water.

15.8 Origin of Methane

The likely source of most of the methane in the Upper Cretaceous Western Interior is biogenic, produced by the decomposition of sedimentary organic matter. The methane probably originated from the organic-rich Pierre Shale and underlying Niobrara Formation, Carlile Shale, Greenhorn Limestone, Belle Fourche Shale, and Mowry Shale, representing a thickness of as much as 1500 m. The low values of $\delta^{13}C$ of the carbonates in the seep deposits are consistent with the anaerobic oxidation of methane (AOM) (Boetius 2000). Birgel et al. (2006) also analyzed the hydrocarbon and fatty acid fraction from samples of limestone in seep deposits from the middle Campanian *Baculites scotti* and upper Campanian *Didymoceras nebrascense* Zones of the Pierre Shale in Colorado. These samples preserve strongly ^{13}C-depleted biomarkers reflecting AOM produced by the consortium of methanotrophic Archaea and sulfate-reducing Bacteria (see Cochran et al. this volume).

In the WIS, the methane likely migrated to the sediment-water interface through a system of faults and fractures acting as a plumbing network. These features probably developed in association with increased tectonic activity during the initiation of the Laramide orogeny starting in the late Campanian. Indeed, Kaufmann et al. (1996) noted that the seep deposits in Colorado trend south-southeast to north-northwest parallel to the Colorado Front Range and Wet Mountains on the west side and southwest-northeast parallel to the Los Animas Arch on the east side. In addition, normal faults may have developed on the sea floor during the early stages of the Laramide orogeny (Tweto 1980). Landman et al. (2012) and Cochran et al. (2015) hypothesized that the seep deposits in the area of eastern Wyoming and western South Dakota originated due to the incipient uplift of the Black Hills during the late Campanian based on the values of $^{87}Sr/^{86}Sr$ in the seep deposits, relative to those in open marine systems at the time. In fact, seep deposits disappear toward the east of the Black Hills even though there is plenty of Pierre Shale, possibly due to the absence of an underlying fault system.

Metz (2010) suggested that the presence of methane seeps in the WIS was related to the position of the broad forebulge depozone in the basin. According to her hypothesis, an increase in the degree of flexure of the forebulge produced a topographic high, causing faults and fractures that promoted the migration of methane. During transgressions, for example, in the middle to late Campanian, the amount of sediment loading would have increased near the orogenic belt, resulting in an increase in the degree of flexure of the forebulge and elevated rates of methane release. In contrast, during regressions, the amount of sediment loading would have decreased near the orogenic belt resulting in a concomitant decrease in the degree of flexure and reduced levels of methane release. However, the idealized model of the foreland basin used by Metz (2010) in her arguments may not be applicable to the late Campanian-early Maastrichtian (see Larson et al. (2014)). Instead, the basin may have been subdivided into multiple fault blocks at this time in association with a change in the angle of subduction of the Farallon Plate (Cross 1986).

15.9 Seep Duration

During the deposition of the Pierre Shale, seep activity persisted from the middle Campanian *Baculites perplexus* Zone to the lower Maastrichtian *B. baculus* Zone, and possibly up to the *B. clinolobatus* Zone, spanning at least 6 Myr (Fig. 15.2). This may represent one of the longest known intervals of seep activity within a single basin in Earth history (see Hryniewicz this volume, for a compilation of fossil seeps of the world).

The temporal duration of a single seep in the WIS is difficult to determine. The most reliable way is to examine the ammonites (and inoceramids) at the bottom and top of a seep deposit to evaluate if they belong to the same or different biozone. The absolute ages of biozones are reasonably well constrained by radiometric dating of

bentonite beds (e.g., Cobban et al. (2006), Merewether and McKinney (2015), Landman et al. (2018a, b, 2020)).

AMNH loc. 3342 in Fall River County, South Dakota, is a grass-covered seep deposit 30 m high that exposes carbonates on the bottom and top. The fossils at the bottom belong to the *Baculites scotti* Zone, and the fossils at the top belong to the *Didymoceras nebrascense* Zone. The difference in age between these two zones equals 0.51 ± 0.34 Myr based on the radiometric ages published in Cobban et al. (2006). AMNH loc. 3812 in Custer County, South Dakota, is a seep deposit that forms a long ridge approximately 100 m in length with a lower mound at one end and a higher mound on the other end, so that the total difference in height between them is approximately 10 m (Fig. 15.3c). The fossils at the bottom belong to the *D. cheyennense* Zone, and the fossils on the top belong to the *B. compressus* Zone, corresponding to an age difference of 0.88 ± 0.39 Myr, based on the radiometric ages published in Cobban et al. (2006). Thus, the seep deposits at both sites span part or all of two ammonite zones, implying that seep activity may have lasted for as long as 0.5–0.9 million years.

15.10 Seep Structure and Faunal Distribution

Studies of the seep deposits in the Upper Cretaceous Western Interior reveal broad variation in seep structure and faunal composition. The structure of the seep deposits from the *Baculites scotti-Didymoceras nebrascense* Zones of the Pierre Shale in Colorado has been extensively studied by Howe (1987) and Kauffman et al. (1996) (see also Arthur et al. (1982), Howe and Kauffman (1986), Kauffman et al. (1990), Bishop and Williams (2000), Bash et al. (2005), Dahl et al. (2005), Anderson et al. (2005), and Larson et al. (2014)). Based on samples of in situ limestone blocks extracted from the seep deposits, they assembled a hypothetical model of seep structure featuring five faunal rings surrounding a central core (Fig. 15.10). The central part of the seep ("spring core facies") consists of a micritic, vuggy, peloidal limestone containing few fossils, mostly reworked lucinids, and a network of anastomosing burrows. Howe (1987) illustrated this facies in cross section as a continuous vertical deposit that interfingers with the surrounding shale.

The "spring core facies" is surrounded by a vuggy, peloidal limestone facies that Howe (1987) called the "*Nymphalucina* coquina." It contains a monospecific assemblage of lucinids in life position, many of which are hollow. The fact that the lucinids are preserved in life position suggests that they lived at the site and were buried in place (Fig. 15.10). The aragonitic shells of the lucinids have been replaced by clear blocky calcite and patches of fibrous chert (Krause et al. 2009). The interiors of the valves have been filled with geopetal structures consisting of peloidal grainstone and fibrous, botryoidal, magnesium (Mg)-rich calcite and clear, blocky, ferroan calcite spar (Fig. 15.11). The lucinids are encased in peloidal grainstone and fibrous, botryoidal, magnesium-rich calcite.

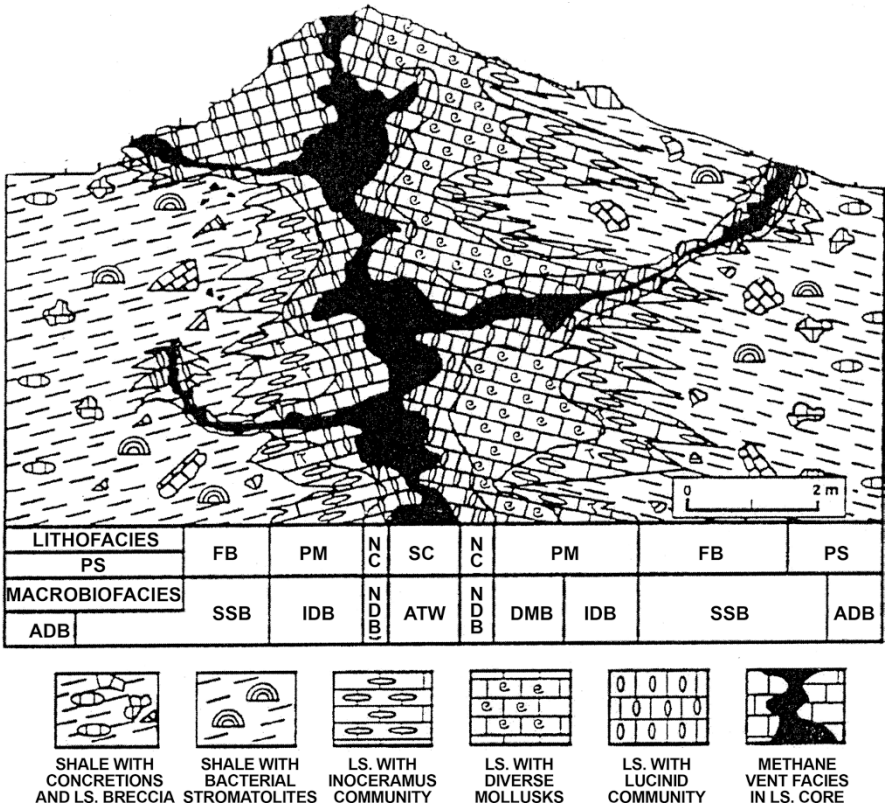

Fig. 15.10 Idealized cross section of a methane seep deposit in Colorado. Abbreviations: Lithofacies: *SC* spring core facies, *NC Nymphalucina* coquina, *PM* peloidal micrite facies, *FB* flank breccias in shale, *PS* concretionary Pierre Shale surrounding mound. Macrobiofacies (bottom): *ATW* agglutinated tube worm biofacies in vents, *NDB Nymphalucina*-dominated biofacies, *DMB* diverse molluscan biofacies, *IDB Inoceramus*-dominated biofacies, *SSB* bacterial (?) stromatolite-serpulid worm biofacies in proximal shales, *ADB* ammonite-dominated biofacies, with small bivalves and gastropods in concretions surrounding deposit (modified from Kauffman et al. (1996), used by permission of the Geological Society of America)

The "*Nymphalucina* coquina" is surrounded by the "brecciated facies," which is surrounded, in turn, by the "middle flank facies," both of which comprise most of the rest of the deposits and contain extensively recrystallized shell material (Fig. 15.10). At some sites, the middle flank facies borders the brecciated facies on the outside, but at other sites, the reverse is true. Both facies are vuggy with peloidal micrite. They contain lucinids, generally not in life position, and a diverse assemblage of other mollusks including ammonites, inoceramids, and gastropods. Some of the lucinids are fragmentary and occur in horizontal beds.

Both of these facies, and especially the brecciated facies, are characterized by fractures and micritic clasts. According to Shapiro and Fricke (2002), authigenic carbonates in seep deposits consist of a variety of fabrics that must have developed

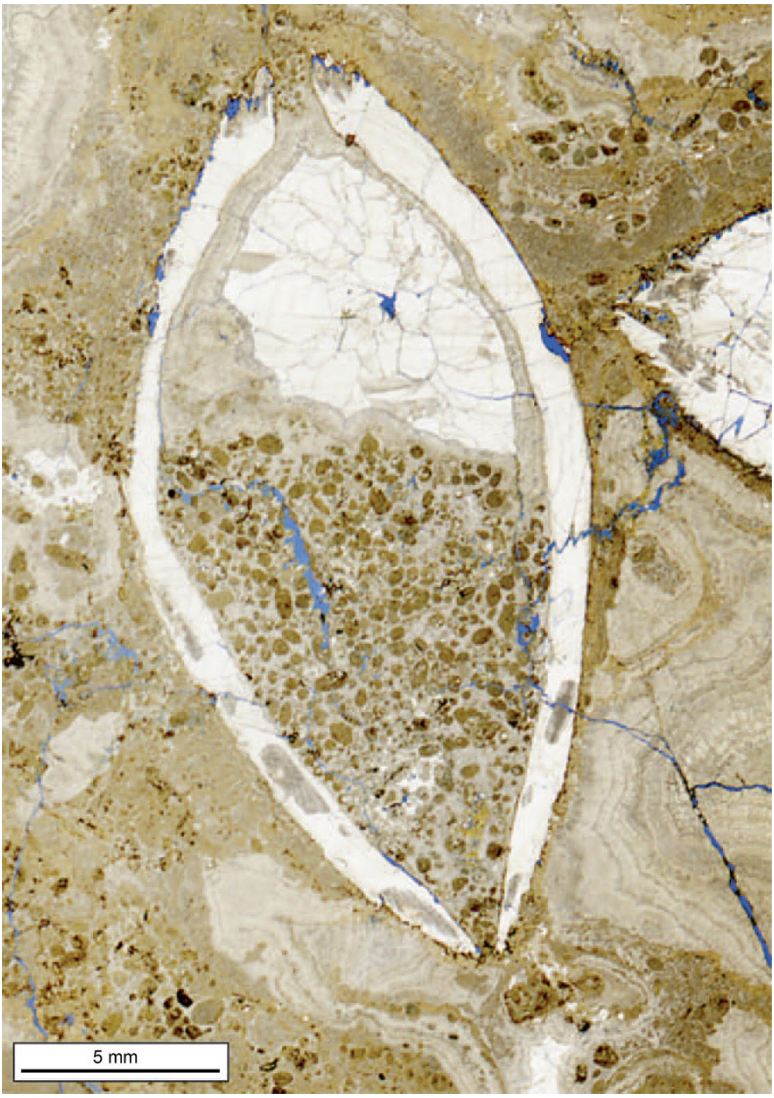

Fig. 15.11 Thin section of a lucinid from a seep deposit in the *Baculites scotti-Didymoceras nebrascense* Zones of the Pierre Shale, Colorado. (Modified from Krause et al. (2009))

at different times during diagenesis (see Hryniewicz et al. this volume). Several generations of early diagenetic cements reflect multiple episodes of dissolution (corrosion) and brecciation. The pelloids are the products of microbial activity or, more likely, fecal activity (Kiel, pers. comm., 2020). They are uncompacted and enclosed by fibrous to bladed calcite cements. The vugs are also lined with multiple generations of cements. Cracks in the micrite are filled with cements or intraclasts derived from the micrite.

Finally, Howe (1987) documented an "oncolite-mud" facies at the margins of the limestone (Fig. 15.10). It consists of abundant, small, irregular masses that Kauffman et al. (1996) identified as stromatolites. The masses are associated with large patchy areas of micrite with irregular, ragged edges. Howe (1987) also documented small pipes, tubes, and irregular limestone structures in the surrounding shale that Cochran et al. (2015) subsequently called "seep-associated concretions" (SACs). In addition, Howe (1987) noted what she called "slump blocks of limestone core and flank facies" in the surrounding shale and remarked that "the bedding of these slump blocks was disjunct with that of the surrounding shale." The faunal community in the surrounding shale is depauperate, dominated by inoceramids, but also contains lucinids and gastropods.

The structure of the seep deposits in Colorado has not been studied in detail since Howe (1987) and Kauffman et al. (1996). Seep deposits of approximately the same age (*Baculites scotti-Didymoceras nebrascense* Zones) are present around the Black Hills (South Dakota, Montana, Nebraska, and Wyoming). These deposits share many of the same structural features documented by Howe (1987). The most conspicuous among them are large masses of vuggy limestone consisting of peloidal micrite. The limestone contains whole and broken fossils, small clasts, and early diagenetic cements forming a porous, clotted texture. However, the concentric pattern of zonation of the facies observed in Colorado is not apparent.

For example, at AMNH loc. 3440, near Newell, Butte County, South Dakota, a large carbonate mass (the main carbonate body or "spring core facies") holds up the top of the deposit (Fig. 15.5a, b). The sides of the mound are covered with irregular pieces of vuggy, peloidal limestone containing abundant and diverse fossils. Numerous articulated lucinids are present, many of which are hollow. Similarly, at AMNH loc. 3386 in Butte County, South Dakota, the limestone is a biomicrite with large vugs up to 1.5 cm long. Lucinids are abundant and articulated, although not in life position, and are accompanied by a variety of other fossils including inoceramids and ammonites (Meehan and Landman 2016). Many lucinids as well as the phragmocones of ammonites are hollow, suggesting rapid burial and cementation before compaction. In addition, ammonite jaws are present, suggesting little transport after the death of the animals, followed by rapid burial (Landman et al. 2013).

The seep deposits from the *Baculites baculus* Zone of the Pierre Shale in Dawson County, Montana (AMNH loc. 3911), also feature large masses of vuggy limestone (Ryan et al. 2020). These deposits are of limited extent (2 m in diameter by 3 m in height) and consist of fossiliferous, peloidal limestone with few SACs. The fauna is dominated by lucinids, most of which are hollow, but also includes a wide variety of other species such as scaphites, nostoceratids, scaphopods, and echinoids. No concentric pattern of faunal distribution is apparent.

Studies of other seep deposits in the Pierre Shale reveal additional variation in seep structure and faunal distribution, which undoubtedly reflects variation in the concentration of methane in seep fluids and the rate and duration of methane emissions. In deposits from the *Didymoceras cheyennense* to *Baculites cuneatus* Zones in South Dakota, the main carbonate bodies are massive, with few vugs. They appear as globular, billowing, micritic limestones ranging up to 3 m in diameter and

up to 3 m in height. They widen and narrow up section and contain few fossils but are usually surrounded by a large number of fossiliferous SACs that vary in shape and composition (Figs. 15.12, 15.13 and 15.14).

An example of such a deposit is AMNH loc. 3529 from the *Didymoceras cheyennense* Zone of the Pierre Shale, Custer County, South Dakota (Fig. 15.5c). It features a massive, bulbous, micritic limestone body that holds up the top of the mound. The limestone contains a few fossils of inoceramids, lucinids, and baculites. It is surrounded by brown-weathering (oxidized) shale with orange partings that contains hundreds of tabular SACs forming platy, pavement-like coquinites. Most of the fossils occur in the SACs or loose in the weathered shale and consist of fragmentary and whole inoceramid shells as well as lucinids, gastropods, ammonites, crinoids, crustaceans, and asteroids. The SACs are not connected physically to the bulbous carbonate mass nor do they represent detached pieces of it but instead are embedded in the shale. Similar crusts are present at AMNH locs. 3419 and 3420 from the *Baculites compressus* Zone of the Pierre Shale, Custer County, South Dakota (Fig. 15.5d). The accompanying SACs are very fossiliferous and contain inoceramids, scaphites, and many species that require a hard substrate for attachment, such as sponges and crinoids.

The details of seep structure are visible in several deposits that are fortuitously exposed in cross section along river cuts. Study of these exposures further reveals the variation in seep structure among deposits and departures from the model described by Howe et al. (1987) and Kauffman et al. (1996). At AMNH loc. 3418 from the *Didymoceras cheyennense* Zone of the Pierre Shale, Custer County, South Dakota, the light gray bulbous mass is surrounded by dark gray shale (Fig. 15.4c, d). The mass is 2 m in diameter and 2.5 m in height. It is irregular in shape, with a few fossils, and interfingers with the surrounding shale. The sediments immediately surrounding the main body consist of brownish-gray calcareous shale with yellow and orange partings as well as the mineral melanterite, which is a product of pyrite weathering. The shale contains abundant SACs that are elongate and subspherical rather than angular or tabular in shape (Figs. 15.12 and 15.13). They range in size from 1 to 20 cm long, with smooth surfaces.

Landman et al. (2012) carefully documented the distribution of fossils at this site by gridding the outcrop into 1 m^2 quadrants and recording the fossils in each quadrant (Fig. 15.13). The fossil distribution does not conform to the concentric zonation model proposed by Howe (1987) and Kauffman et al. (1996). Lucinids, inoceramids, scaphites, and baculites are more abundant on the north side of the carbonate body at lower horizons and more abundant on the south side of the carbonate body at higher horizons, coinciding with the abundance of SACs in each area. This asymmetric distribution may reflect the fact that the locus of methane emission changed from the north to the south side of the site over time. Gastropods, although limited in number, are more abundant on the north side, and didymoceratids and spiroxybeloceratids are more abundant in the middle of the exposure. In areas of shale devoid of SACs, the only shelled organisms are inoceramids.

Fossils at this site extend up to a distance of 5 m on either side of the large carbonate mass and are usually preserved in three dimensions with their original

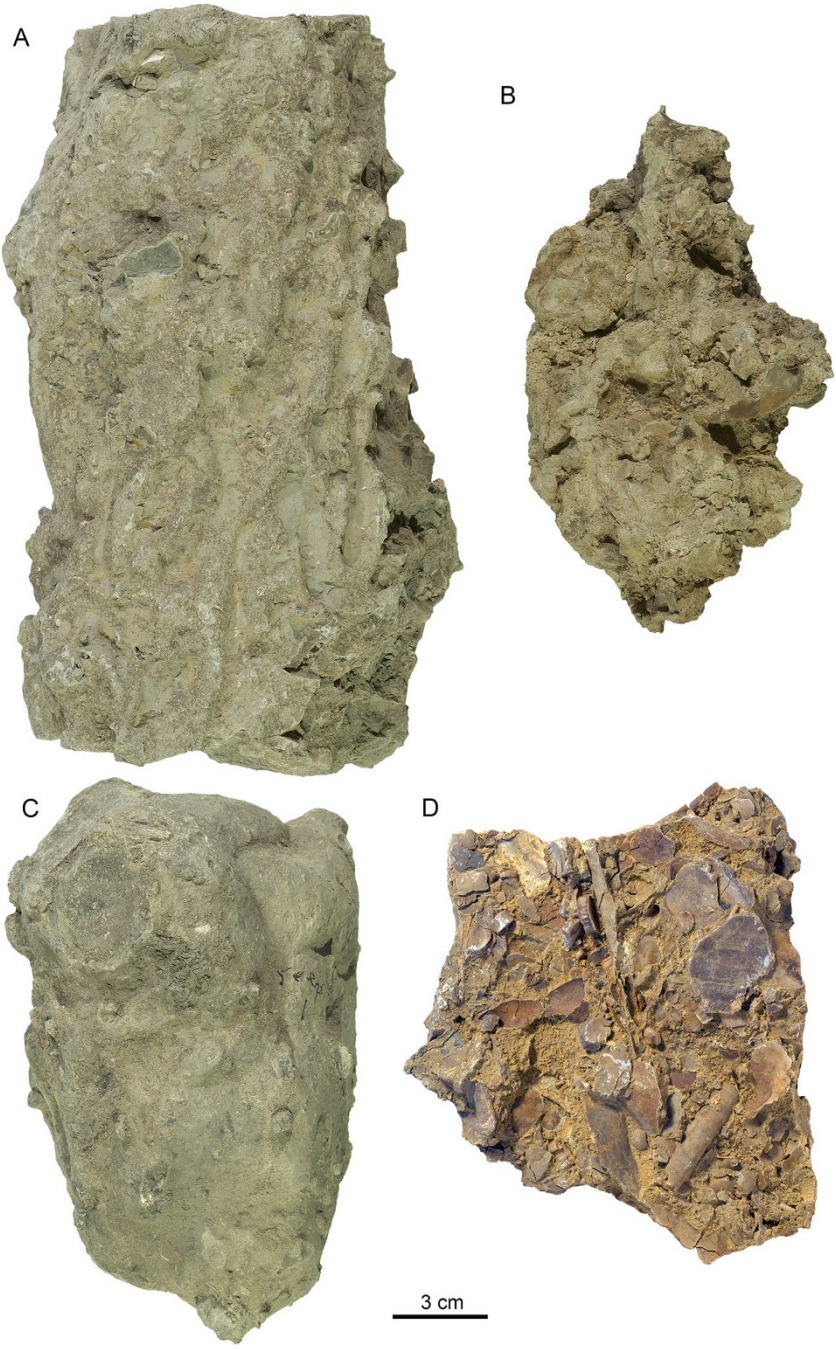

Fig. 15.12 SACs (seep-associated concretions) from seep deposits in the Pierre Shale of South Dakota (reprinted from Cochran et al. (2015); http://creativecommons.org/licenses/by/4.0/). (**a**) Portion of a large pipe 30 cm long x 10 cm diameter composed of Mg-rich calcite with apatite and pyrite (AMNH 64594, AMNH loc. 3545, Meade County). (**b**) Irregular SAC (AMNH 80770, AMNH loc. 3419, Custer County). (**c**) Subspherical SAC (AMNH 645611, AMNH loc. 3528, Meade County). (**d**) Platy SAC (top view) containing inoceramids and lucinids (AMNH 108407, AMNH loc. 3529, Pennington County)

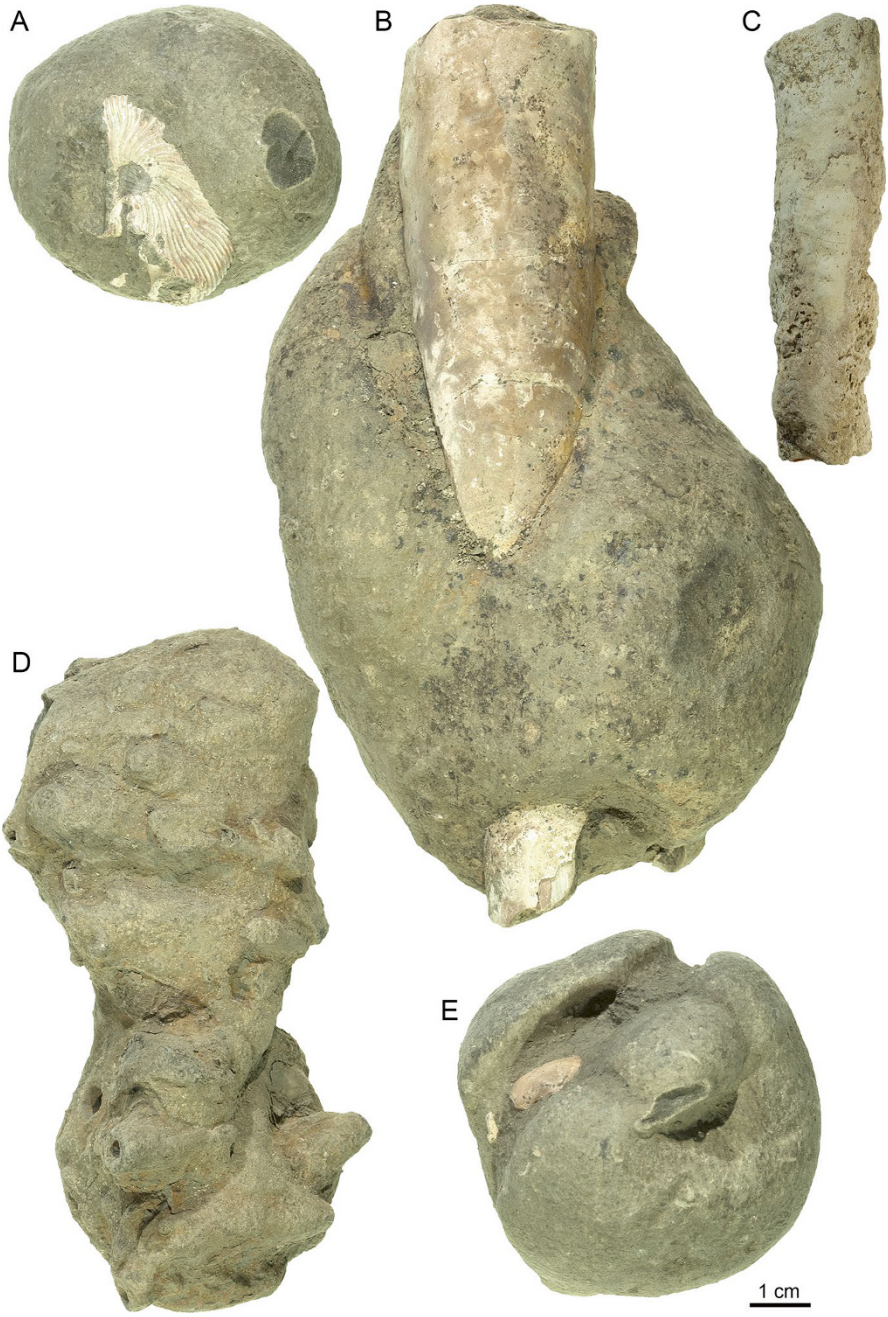

Fig. 15.13 SACs (seep-associated concretions) and tubes from seep deposits in the Pierre Shale, South Dakota. (**a**, **b**, **e**) Subspherical SACs from AMNH loc. 3528, Meade County, composed of Mg-rich calcite with minor amounts of apatite and pyrite containing well-preserved specimens of scaphites (**a**: AMNH 64625), baculites (**b**: AMNH 64595), and lucinids (**e**: AMNH 64623). (**c**) Small pipe-like SAC (AMNH 64608, AMNH loc. 3528, Meade County). (**d**) Tube (AMNH 79109, AMNH loc. 3418, Custer County). (Reprinted from Cochran et al. (2015); http://creativecommons.org/licenses/by/4.0/)

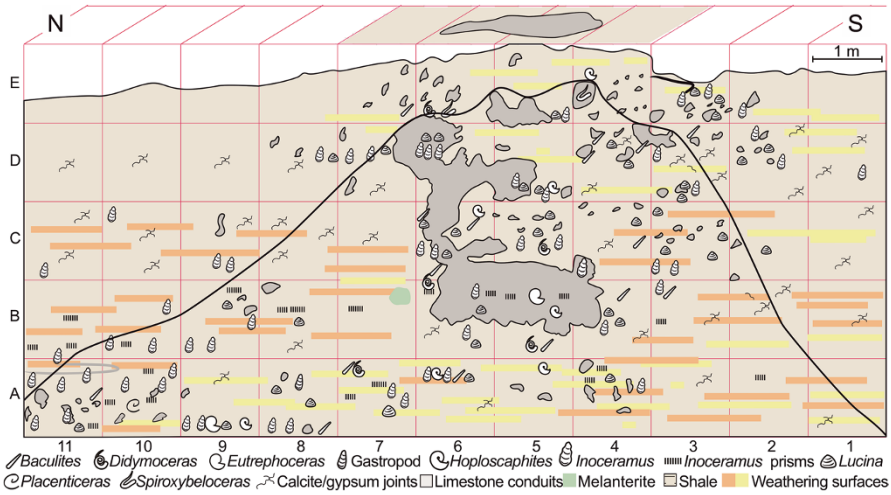

Fig. 15.14 Cross section of a seep deposit in the Pierre Shale, *Didymoceras cheyennense* Zone, AMNH loc. 3418, Custer County, South Dakota. The thin black outline indicates the probable shape of the seep deposit if it were eroded back, with the resistant carbonate masses holding up the top of the mound, forming a tepee butte. (Modified from Landman et al. (2012), used by permission of the Geological Society of America)

mineralogy. They occur throughout the section but are more common at some horizons than others. The most abundant fossils are lucinids and inoceramids that occasionally form crushed, flattened accumulations. All of the lucinids are articulated indicating little transport after death. The shale on the outer margins of the seep deposit, up to 20 m away, is much darker gray, with fewer or no fossils, more typical of the Pierre Shale at non-seep sites. The thin black outline shown in Fig. 15.14 indicates the likely shape of this seep deposit if the surrounding shales were weathered back, leaving the resistant carbonate masses holding up the top of the mound and forming a tepee butte-like seep deposit.

AMNH loc. 3545 from the *Baculites compressus-B. cuneatus* Zones of the Pierre Shale, Meade County, South Dakota, is also exposed in cross section. It features a large carbonate body consisting of several globular masses, which are sparsely fossiliferous. The shale immediately surrounding the carbonate body (up to a distance of approximately 2 m) preserves a rich assemblage of crushed and non-crushed molluscan shells, which retain their original mineralogy. The shale also contains large, massive pipe-like SACs ranging from 10 cm in length and 1 cm in diameter to 40 cm in length and 10 cm in diameter (Fig. 15.12), as well as smaller, hollow tubes with granular outer surfaces, which may have originally formed as crustacean burrows but were subsequently utilized as conduits for methane flow (see below). As shown in thin section, these pipe-like SACs are composed of carbonate-cemented shale filled with pelloids. They also exhibit brecciated features, indicating breakage and re-cementation of the material in the pipes. Subspherical- or dumbbell-shaped SACs are also present in the shale and occasionally bear one or two fossils such as

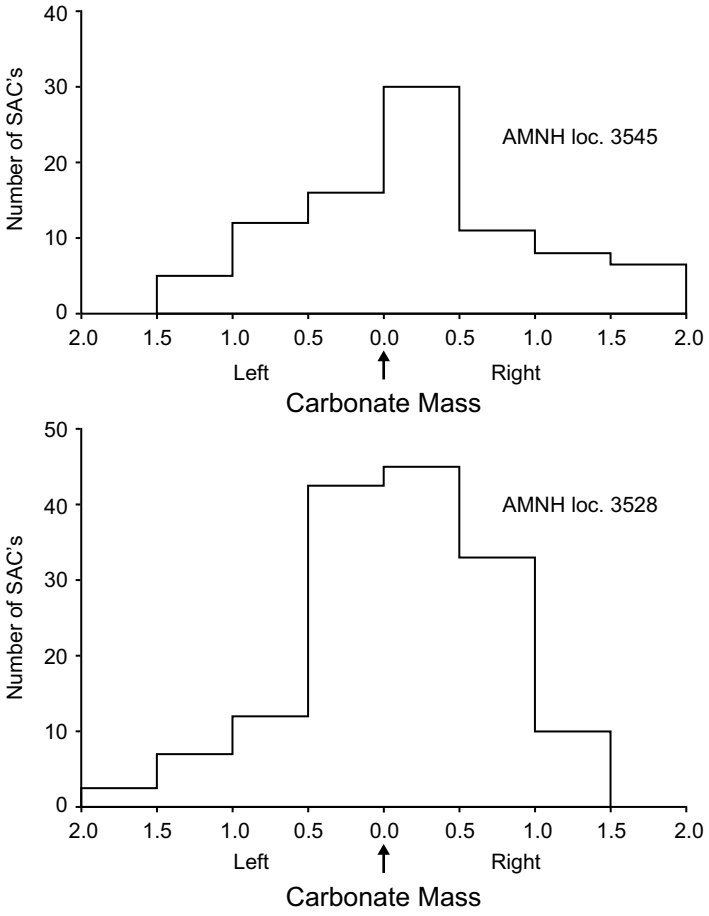

Fig. 15.15 Distribution of seep-associated concretions (SACs) relative to the main carbonate body (centered at 0) at two seep deposits in the Pierre Shale of South Dakota (measurements by M. Garb and A. Rashkova)

baculites and scaphites. The SACs abruptly disappear within a distance of approximately 1–2 m of the main carbonate body (Fig. 15.15).

15.11 Faunal Composition

15.11.1 Abundance and Diversity

The most striking feature of the seep deposits in the Western Interior of North America is the abundance of organisms at these sites relative to their paucity in the surrounding shale. This is not simply a taphonomic artifact due to preferential

preservation in carbonate concretions. In fact, many of the fossils in seep deposits are preserved in the shale itself, immediately adjacent to the carbonate masses, rather than in concretions. The shale surrounding the seep deposits (10s of meters away) yields few or no fossils. As noted above, at AMNH loc. 3418, the shale on the outer margins of the seep deposit (10–20 m away) is much darker and contains few or no fossils (Fig. 15.14).

The fauna in the seep deposits from the Cenomanian Tropic Shale in Utah has been described by Kiel et al. (2012) and includes a variety of bivalves (inoceramids, lucinids, solemyids, and arcoids), opisthobranch gastropods, serpulid worm tubes, and ammonites. The fauna in the seep deposits from the lower Campanian Ojinaga Formation in Texas has been described by Metz (2002) and includes bivalves (inoceramids, *Exogyra*, and *Cyprimeria*), ammonites (*Placenticeras*), gastropods, and small solitary corals. The fauna in the seep deposits from the Campanian-Maastrichtian Pierre Shale in Colorado, Wyoming, South Dakota, Nebraska, and Montana includes inoceramids, lucinids, gastropods, crinoids, nautilids (*Eutrephoceras*), ammonites (*Solenoceras*, *Menuites*, *Baculites*, *Hoploscaphites*, *Placenticeras*, *Didymoceras*, and *Spiroxybeloceras*), irregular and regular echinoids, asteroids, crabs, ophiuroids, shrimp, sponges, corals, serpulid worm tubes, algae, foraminifera (both planktonic and benthic species comprising calcareous, agglutinated, and arenaceous forms), radiolaria, bryozoa, fish, sharks, and reptiles (Figs. 15.16, 15.17, 15.18, 15.19 and 15.20; Howe 1987; Kauffman et al. 1996; Bishop and Williams 2000; Landman et al. 2012, 2013; Larson et al. 2014; Meehan and Landman 2016; Hunter et al. 2016; Blake et al. 2018; Thuy et al. 2018; Laird and Belanger 2018; Meehan et al. 2018; Ryan et al. 2020). In addition, the seep system must have contained abundant organic matter in the form of phytoplankton and zooplankton, which are not preserved as fossils and which must have afforded an abundant source of food for other animals.

The seeps also hosted a large microbial community. Shapiro and Fricke (2002: Fig. 6) examined the seep deposits from the Campanian of Colorado and identified possible microbial filaments consisting of agglomerations of cocci and straight and curved rods 0.5–1 μm in diameter. They occur in the pelloids and are associated with framboidal pyrite (Shapiro 2004; Shapiro and Gale 2001). Thus, the entire framework of the seep limestones may have represented a thrombolytic microbialite, reflecting the original microbial ecosystem (for further details, see Shapiro this volume). Indeed, Birgel et al. (2006) reported biomarkers in these deposits indicative of sulfate-reducing bacteria that mediated the anaerobic oxidation of methane. In addition, bacterial mats are present, which reveal fine laminations in cross section (Fig. 15.19r, v).

It is important to note, however, that many seep deposits in the WIS are devoid of macrofossils. For example, in the area near Oelrichs, Fall River County, South Dakota, in which Darton (1902) mapped hundreds of seep deposits, we estimate that 7–10% of them lack macrofossils (Fig. 15.8). The presence of large masses of limestone indicates the precipitation of authigenic calcium carbonate. However, it is possible that the methane in these seeps did not reach the sediment-water interface and, therefore, did not support a seep ecosystem. In addition, the levels of oxygen

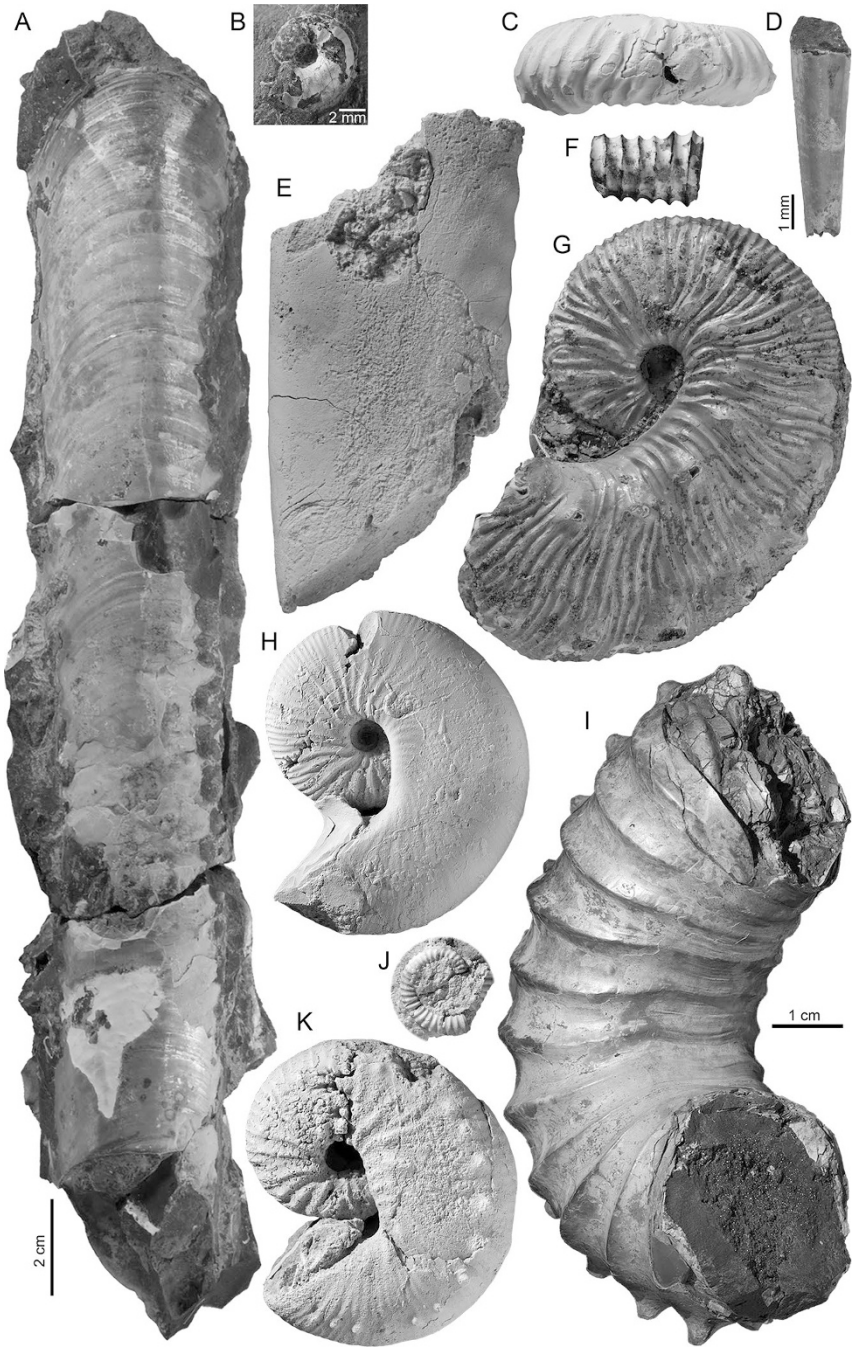

Fig. 15.16 Ammonite fauna in methane seep deposits in the Campanian Pierre Shale, South Dakota and Wyoming. (**a**) *Baculites corrugatus* Elias, 1933, mature macroconch, ventral view,

(continued)

may have been too low, and/or the concentrations of hydrogen sulfide may have been too high to sustain life.

15.11.2 Background Taxa

Most species in the seep deposits in the WIS reflect the background fauna and are not seep-obligate (Kiel et al. 2012; Meehan and Landman 2016). In general, the fauna is abundant but not diverse, with a few species usually being dominant. In the seep deposits from the Campanian-Maastrichtian Pierre Shale, the dominant macroinvertebrates are lucinids (sometimes almost exclusively), tube worms, baculites, and inoceramids (Kauffman et al. 1996; Laird and Belanger 2018). For example, at AMNH loc. 3489 from the *Didymoceras cheyennense* Zone of the Pierre Shale in Custer County, South Dakota, Meehan and Landman (2016) documented that baculites, inoceramids, and lucinids comprise 90.9% of the total number of organisms sampled (n = 197), suggesting that these organisms formed the "foundation" of the seep ecosystem. For a counter example, a seep deposit from the *Baculites jenseni* Zone of Musselshell County, Montana (WPT 69), is dominated by lucinids and baculites, but no inoceramids.

Because all of the seeps in the WIS developed in relatively shallow water (see below), any differences in faunal abundance among them are not due to variation in water depth. This contrasts with observations of modern seeps in which variation in water depth is an important factor in explaining differences in faunal abundance. For example, Sahling et al. (2003) documented that faunal diversity decreases with increasing depth in seep communities in the Sea of Okhotsk in the western Pacific Ocean. In the WIS, in contrast, differences in faunal abundance among seeps are more likely due to variations in the chemical gradients on the sea floor and in the overlying water column, reflecting the persistence and rate of methane flow and the concentrations of oxygen and hydrogen sulfide. The other important factor

with aperture on the top, AMNH 58552, AMNH loc. 3418. (**b**) *Hoploscaphites brevis* (Meek 1876), juvenile, left lateral view, AMNH 66244, AMNH loc. 3418. (**c**) *Didymoceras cheyennense* (Meek and Hayden 1856), fragment, AMNH 63440, AMNH loc. 3418. (**d**) *Baculites* sp., juvenile, lateral view, AMNH 112942, AMNH loc. 3545. (**e**) *Baculites compressus* Say, 1820, right lateral view, AMNH 58544, AMNH loc. 3419. (**f**) *Spiroxybeloceras meekanum* (Whitfield 1877), fragment, AMNH 66289, AMNH loc. 3418. (**g**) *Hoploscaphites brevis* (Meek 1876), mature microconch, left lateral view, AMNH 66275, AMNH loc. 3418. (**h**) *Hoploscaphites gilli* Cobban and Jeletzky 1965, mature macroconch, left lateral view, USNM 547334, USGS Mesozoic loc. D1900, *B. scotti-D. nebrascense* Zones, Niobrara County, Wyoming (non-seep site, but species is also present at age-equivalent seep sites). (**i**) *Didymoceras cheyennense* (Meek and Hayden 1856), AMNH 102504, AMNH loc. 3489, *D. cheyennense* Zone, Pennington County, South Dakota (non-seep site, but species is also present at age-equivalent seep sites). (**j**) *Didymoceras cheyennense* (Meek and Hayden 1856), early whorls, AMNH 82739, AMNH loc. 3529. (**k**) *Hoploscaphites gilberti* Landman et al. 2014, mature macroconch, left lateral view, AMNH 83717, AMNH loc. 3386. The 1 cm scale bar on the bottom applies to all specimens except **a**, **b**, and **d**

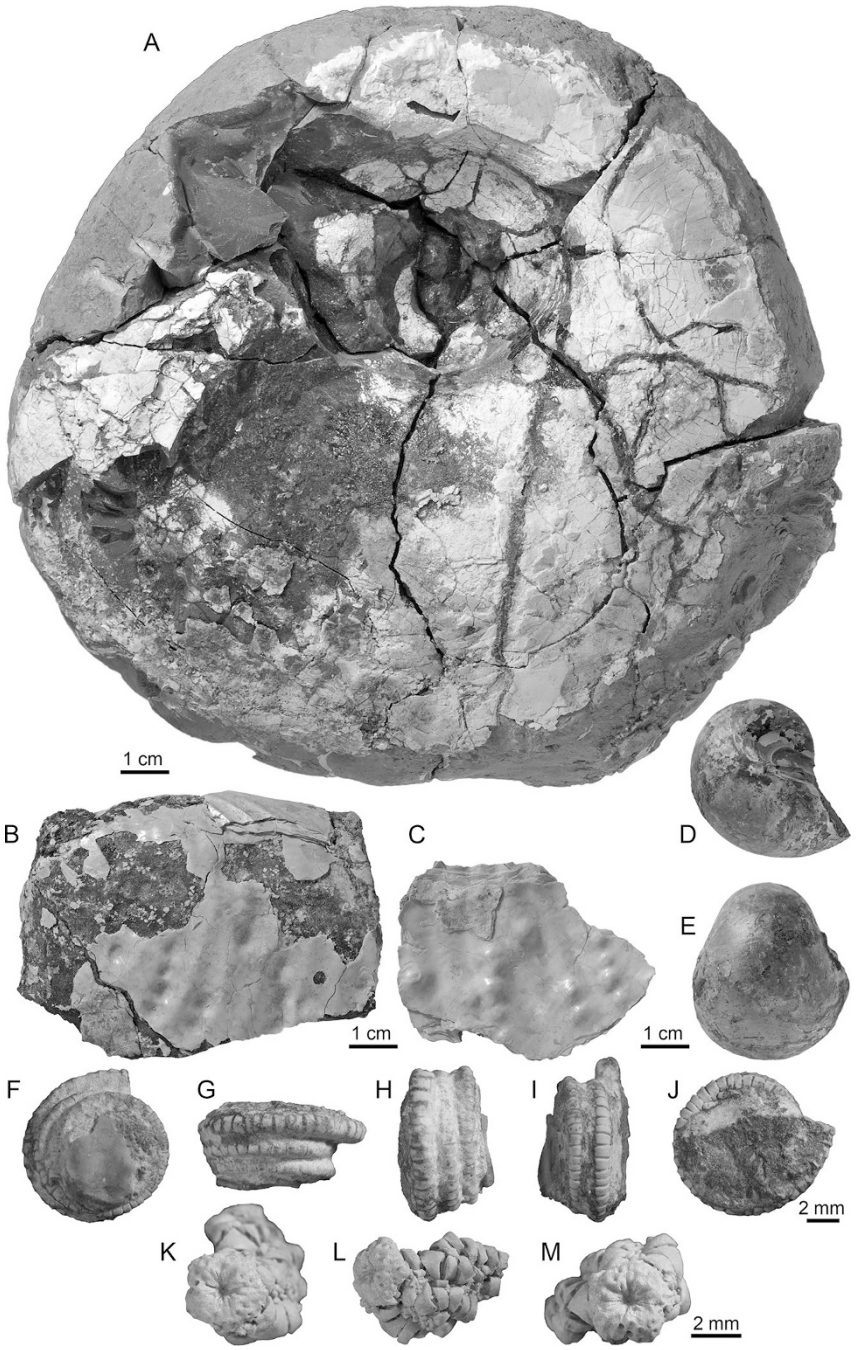

Fig. 15.17 Fauna in methane seep deposits in the Campanian Pierre Shale, South Dakota. (**a**) *Pachydiscus* sp., left lateral view, AMNH 105841, AMNH loc. 3528. (**b**, **c**) Fragment of *Inoceramus* sp., with an infestation of blister pearls, AMNH 108328, AMNH loc. 3528. (**d**, **e**) Right lateral and ventral views of *Eutrephoceras dekayi* (Morton 1834), AMNH 63647, AMNH loc. 3545. (**f–j**) Curled arm of a crinoid, probably *Lakotacrinus brezinai* Hunter et al. 2016, five views, AMNH 161015, AMNH loc. 3507. (**k**–**m**). Crown of a comatulid (feather star), possibly *Glenotremites*, three views, AMNH 161016, AMNH loc. 3529

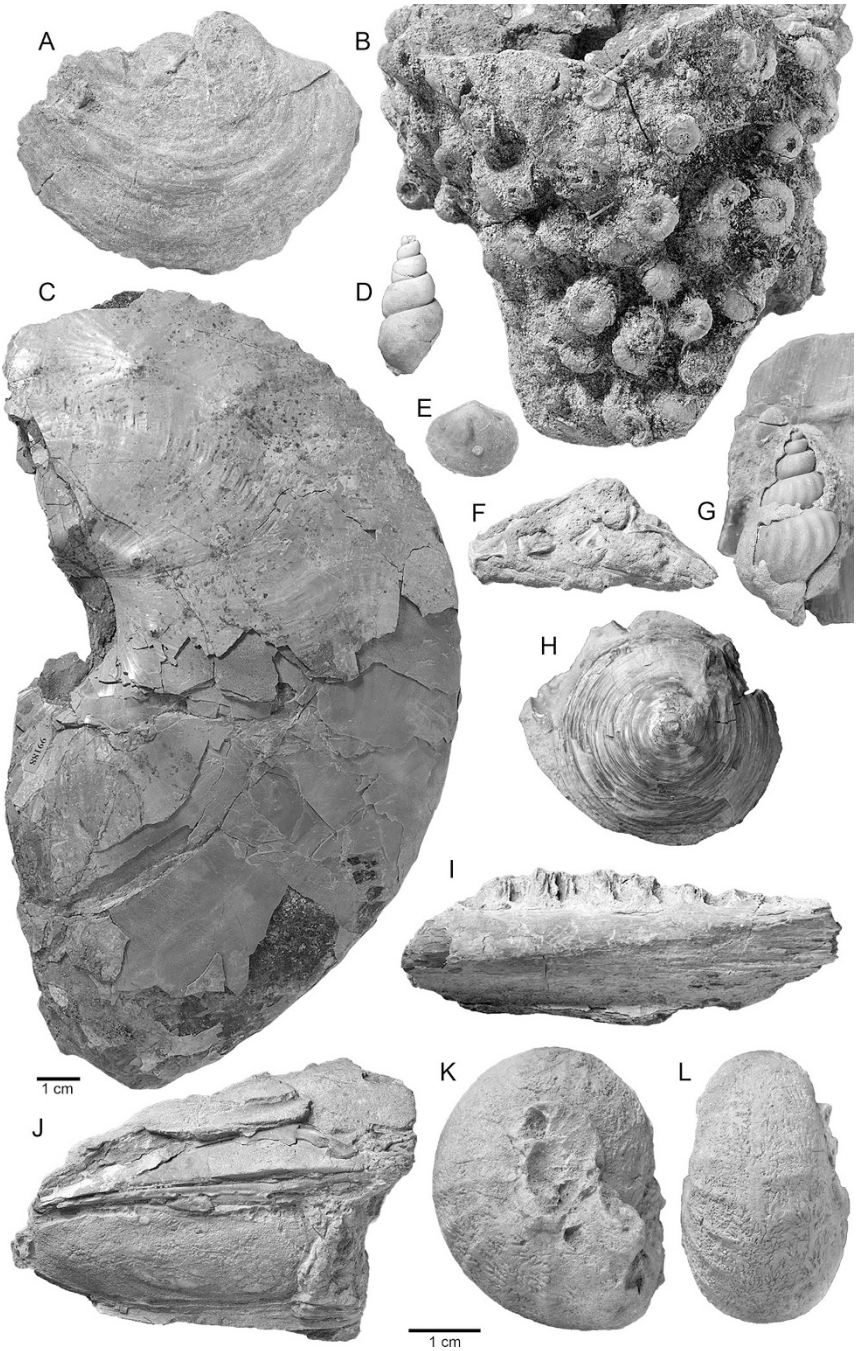

Fig. 15.18 Fauna in methane seep deposits in the Campanian Pierre Shale, South Dakota, and Nebraska. (**a)** *Ostrea* sp., AMNH 82749, AMNH loc. 3529. (**b)** Echinoids, AMNH 82716, AMNH loc. 3654. (**c)** *Placenticeras costatum* Hyatt 1903, left lateral view, AMNH 99188, AMNH loc. 3545. (**d)** *Drepanochilus* sp., AMNH 82750, AMNH loc. 3529. (**e)** Bivalve, AMNH 82748, AMNH loc. 3529. (**f)** Articulated fish vertebra, AMNH 82743, AMNH loc. 3529. (**g)** *Bellifusis* sp., AMNH 82741, AMNH loc. 3529. (**h**) Fish vertebra, AMNH 82747, AMNH loc. 3686. (**i)** Fish jaw, AMNH 82740, AMNH loc. 3529. (**j**) Fish, unidentified head bones, AMNH 82746, AMNH loc. 3529. (**k**, **l**) *Menuites* sp., AMNH 82737, right and ventral views, AMNH loc. 3666. The 1 cm scale bar on the bottom applies to all specimens except (**c)**

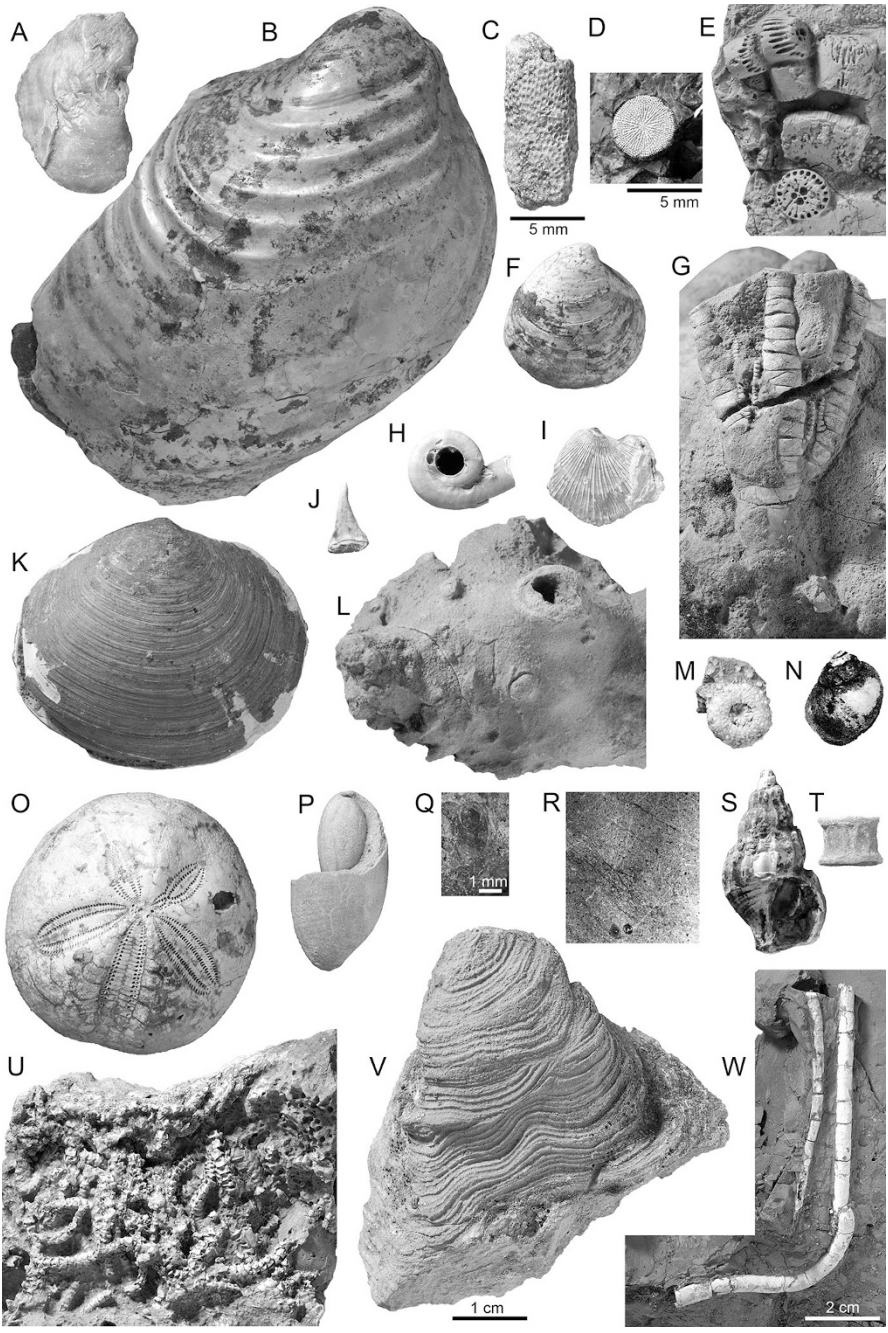

Fig. 15.19 Fauna in methane seep deposits in the Campanian Pierre Shale, South Dakota, and Montana. **(a)** *Ostrea* sp., AMNH 82729, AMNH loc. 3529. **(b)** "*Inoceramus*" *sagensis* Owen 1852, AMNH 66248, AMNH loc. 3418. **(c)** Bryozoan, AMNH 82730, AMNH loc. 3529. **(d)** *Microbacia*

(continued)

controlling faunal abundance and diversity is the nature of the substrate, that is, whether it is a soft, clayey mud or a hard carbonate crust (for a description of a hard ground substrate, see Hunter et al. (2016); for an example of a soft, muddy bottom, see Ryan et al. (2020)). Currents on the sea floor may also have contributed to the development of the seep community, for example, by periodically exposing the carbonate crust, permitting the settlement of oysters and inoceramids (see below).

15.11.3 Hard Ground Taxa

The development of a hard crust at a seep is the result of the authigenic precipitation of calcium carbonate at the sediment-water interface. Such hard grounds provide suitable substrates for animals to colonize, which, in turn, promote further development of the hard substrate. For example, accumulations of large inoceramid shells form broad tabular pavements (1–3 m across) that provide additional surfaces to which animals can attach. This is an example of positive feedback.

The presence of a hard substrate permits the colonization of many species, some of which are unique to these habitats. Such species include stalked articulate crinoids, feather stars, sponges, regular and irregular echinoids, ophiuroids, asteroids, tube worms, crabs, bryozoa, and corals. However, even in seep deposits in which these organisms appear, the background taxa are still dominant (Meehan and Landman 2018). In addition, it is possible that some of these species actually occur elsewhere but are preferentially preserved in the seep deposits. For example, echinoids are, in fact, present in age-equivalent non-seep sites, but they are more difficult to recognize because their tests are commonly broken up due to predation and/or are fused into the fine-grained concretionary matrix (Landman and Klofak 2012).

The distribution of hard ground fauna has been extensively studied at AMNH loc. 3529 from the *Didymoceras cheyennense* Zone of the Pierre Shale, Custer County, South Dakota. Crinoids occur in patches associated with tabular SACs composed of inoceramid valves. If this pattern reflects their original distribution, it suggests that the crinoids were gregarious in life and formed clusters of tens to

sp., AMNH 82731, AMNH loc. 3529. (**e**) Columnals of *Lakotacrinus brezinai* Hunter et al. 2016, AMNH 66260, AMNH loc. 3419. (**f**) *Crassatella evansi* Hall and Meek 1856, AMNH 108491, AMNH loc. 3418. (**g**) Crown of *Lakotacrinus brezinai* Hunter et al. 2016, AMNH 69618, AMNH loc. 3456. (**h**) Serpulid worm tube, AMNH 82732, AMNH loc. 3529. (**i**) *Pecten* sp., AMNH 82733, AMNH loc. 3529. (**j**) Fish tooth, AMNH 82734, AMNH loc. 3529. (**k**) *Nymphalucina occidentalis* (Morton 1842), AMNH 66246, AMNH loc. 3418. (**l**) Sponge, AMNH 66249, AMNH loc. 3419. (**M**) Echinoid, AMNH 82706, AMNH loc. 3509. (**n**) *Euspira obliquata* (Hall and Meek 1856), AMNH 80369, AMNH loc. 3418. (**o**) Echinoid, AMNH 82710, AMNH loc. 3456. (**P**) Gastropod, AMNH 82735, AMNH loc. 3529. (**q**) Lingulid brachiopod, AMNH 116218i, AMNH loc. 3911. (**r**, **v**) Algal mat (stromatolite?), AMNH 82727, surface and cross section, AMNH loc. 3420. (**s**) *Drepanochilus triliratus* Stephenson 1941, AMNH 108492, AMNH loc. 3418. (**t**) Fish vertebra, AMNH 82736, AMNH loc. 3529. (**u**) *Brezinacantha tolis* Thuy et al. 2018, AMNH 113585, AMNH loc. 3509. (**w**) Tube worm, AMNH 82738, AMNH loc. 3528. The 1 cm scale bar on the bottom applies to all specimens except **c**, **d**, **q**, and **w**

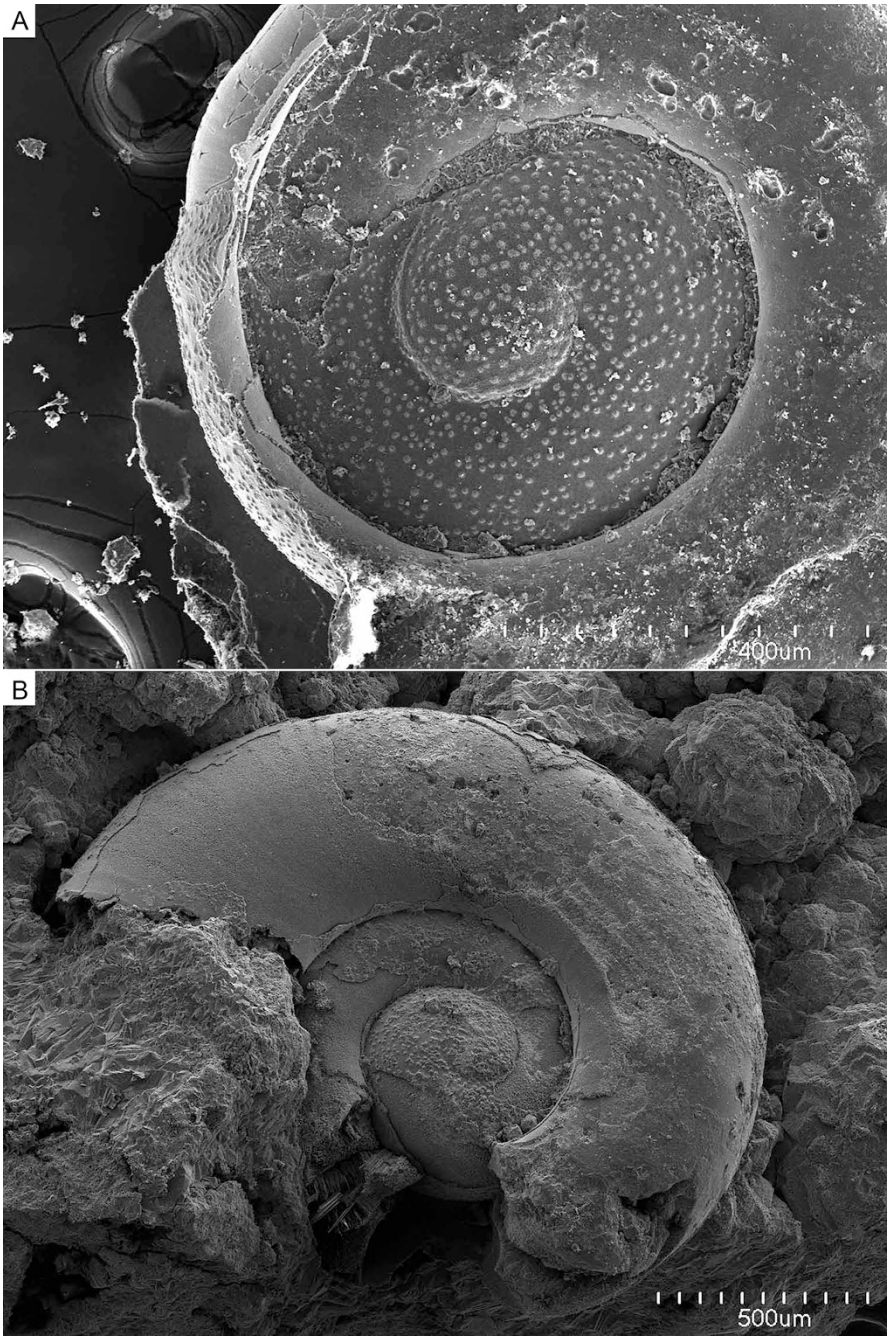

Fig. 15.20 Small juveniles of *Hoploscaphites* preserved in seep deposits, AMNH loc. 3440. A. AMNH 112950. B. AMNH 112949. The tuberculate micro-ornamentation on the embryonic shell is visible. (Photos by A. Rowe)

hundreds of individuals (Hunter et al. 2016). Because these crinoids lack attachment discs or cirri, they probably anchored themselves in the irregular crevices of the substrate. Alternatively, they may have used their long arms for anchoring on the bottom (Hunter et al. 2016). They are preserved either articulated or slightly disarticulated, without any signs of abrasion, indicating that they were buried soon after death, perhaps trapped in bacterial mats. Their preservation was also facilitated by the rapid rate of authigenic precipitation of carbonate at the sediment-water interface.

Asteroids, ophiuroids, and gastropods at this seep site also seem to occur in patches (Blake et al. 2018; Thuy et al. 2018). The hard, crustal substrate probably promoted an increase in habitat complexity, providing small niche-like spaces for such animals as gastropods and echinoids (Meehan and Landman 2016). The remains (claws) of ghost shrimp are also clustered together, associated with concentrations of burrow-shaped SACs. Most intriguingly, certain ammonites such as didymoceratids and spiroxybeloceratids also appear to be more abundant in some areas of this seep deposit than others. If this pattern reflects their original distribution, it suggests that the ammonites homed in on food-rich resources, with important implications for the mode of life of these animals. In contrast, baculites, scaphites, and placenticeratids do not show a preferred distribution but occur everywhere in the deposit. Ultimately, of course, the distribution of organisms at this seep site probably reflects the distribution of food resources, as well as the concentration of O_2 and H_2S in the area.

15.11.4 Ammonites as Seep Inhabitants

Landman et al. (2012, 2018a, b) advanced the hypothesis that ammonites formed an integral part of the seep community, rather than simply representing empty shells that floated in after the death of the animals. They based this hypothesis on both isotopic and paleontologic evidence. Several seep deposits in South Dakota contain exceptionally well-preserved shell material, permitting geochemical analyses of the ammonite shells themselves. The ammonites from seep sites exhibit lower values of $\delta^{13}C$ (as low as −14‰) than ammonites from age-equivalent non-seep sites (as high as 3‰) (see Landman et al. this volume, for further discussion).

The relatively low values of $\delta^{13}C$ of the ammonites from seep sites suggest that they were impacted by a methane-derived ^{12}C-enriched signal in the DIC reservoir above the seep. Indeed, Landman et al. (2018a, b) compared estimates of $\delta^{13}C$ of the DIC reservoir above two seeps in the *Baculites compressus* Zone (−0.7‰) with an age-equivalent non-seep site in the same basin (+2.3‰). The $\delta^{13}C$ of the ammonites may also reflect incorporation of metabolic carbon from the prey that the ammonites ate at the seep. For example, ammonites may have fed on small microorganisms in the water column, such as floating larvae, as documented by Kruta et al. (2011). Such "vital" effects can produce non-equilibrium fractionation in the shell relative to the $\delta^{13}C$ of the DIC reservoir (He et al. 2005; Lukeneder et al. 2010; Tobin and

Ward 2015; Landman et al. 2018a, b). The isotope measurements of Landman et al. (2018) were performed on specimens of the same species (*B. compressus*) from seep and non-seep environments, suggesting that if the fraction of metabolic carbon incorporated into the shell was equivalent at both sites, then the lower values of $\delta^{13}C$ in the seep ammonites were the result of the animals living at the seep.

This hypothesis is reinforced by the $^{87}Sr/^{86}Sr$ isotope ratios of the shells of seep ammonites, which are elevated relative to the coeval sea water values (Landman et al. 2012; Cochran et al. 2015; Cochran et al. this volume). The data suggest that (1) seep fluids likely acquired the elevated values of $^{87}Sr/^{86}Sr$ through reaction with a radiogenic Sr source (the nascent Black Hills granite) at depth in the deposit and (2) these anomalous values of $^{87}Sr/^{86}Sr$ were imprinted on the dissolved Sr in the water above the seep and thus were incorporated into the shells of ammonites living there. The Sr isotope results suggest that seep fluids must have migrated from depth through the overlying muddy sediments via fractures and faults and likely accumulated biogenic methane en route.

In addition to isotopic data, Landman et al. (2010, 2012) documented paleontological evidence that the ammonites preserved in seep deposits in the basin actually lived there and did not float in as empty shells after death. One piece of evidence in support of this interpretation is that the ammonites preserved in seep deposits occur as both adults and juveniles, including newly hatched individuals (Fig. 15.20). In fact, the abundance of small juveniles in some deposits suggests that these sites acted as ammonite nurseries (Rowe et al. 2020). In addition, in ammonites in which sexual dimorphism can be recognized, both dimorphs (presumably the males and females) occur in the same seep deposit. Because ammonites, like modern cephalopods, probably congregated en masse for reproductive purposes, the presence of both sexes implies the existence of a breeding population (Landman et al. 2010). Furthermore, ammonite jaws, comprising upper and lower mandibles, are also present in seep deposits. Jaws are very delicate structures, and their preservation implies that the ammonites did not float into the site after death. Finally, many ammonites at seep sites exhibit lethal injuries, as indicated by missing portions of shell material from the adapical end of the body chamber. These injuries probably occurred at the seep sites, suggesting that ammonites formed an integral part of the seep food web.

The isotopic composition of echinoderms has also been investigated for clues about their mode of life. Kato et al. (2017) analyzed the carbon isotopic composition of crinoids from seep deposits in the upper Campanian Pierre Shale. The skeletons of these specimens are well preserved with little or no diagenetic alteration. The microstructure is intact, and the concentration of Mg is similar to that in modern echinoderms and much higher than that in the surrounding shale matrix. The values of $\delta^{13}C$ of the skeletal material are very low and range from −32‰ to −11‰. Therefore, as with the ammonites, these low values suggest that the crinoids lived at the seep and incorporated a light carbon isotopic signature in their skeletons (for counter arguments, see Hunter et al. (2018) and Kato et al. (2018)).

15.11.5 Cognate Community

As documented by Brezina et al. (2019), a large log was discovered in the upper Campanian Pierre Shale in Custer County, South Dakota, near AMNH loc. 3504 (Fig. 15.21). The whole region is peppered with seep deposits and probably comprised a seep field. The log is 2.8 m long and preserved in a concretion 3.4 m long. The concretion also contains scaphites and baculites. The surface of the log is covered with a thin crust of bivalves, which represents a wood fall association. The log is oriented east-west, possibly reflecting the prevailing currents, and may have come to rest in a depression on the sea floor. Although wood is not uncommon in the Pierre Shale, most of it consists of small fragments, which are not associated with a wood fall fauna.

15.12 Paleoenvironment at the Seep

15.12.1 Migration of Methane

As noted above, the low values of $\delta^{13}C$ of the limestones in the Upper Cretaceous US Western Interior seep deposits indicate that methane was the primary source of carbon. In addition, Birgel et al. (2006) studied the molecular fossils preserved in the limestones from the Campanian seep deposits in Colorado. They documented ^{13}C-depleted archaeal lipids that were derived from anaerobic oxidation of methane (AOM). They also reported a suite of ^{13}C-depleted biomarkers indicating the former presence of sulfate-reducing bacteria. These bacteria are part of the consortium of Archaea and Bacteria that account for one of the principal pathways of AOM.

Methane may have migrated to the sediment-water interface through diffusion and advection along fractures in the fine, unconsolidated sediments. Methane may also have reached the overlying water column via preexisting, relic burrow networks that were exapted for methane conduits (Krause et al. 2009; Wiese et al. 2015; Cochran et al. 2015; Cochran et al. this volume). The tubes in the seep deposits in the Campanian Pierre Shale of Colorado were initially attributed to vestimentiferan and pogonophoran tube worms, but it is more likely that they were crustacean burrows. For example, at AMNH loc. 3344 near Newell, Butte County, South Dakota (Fig. 15.3d), the main carbonate body contains anastomosing hollow tubes, which probably represent the burrows of ghost shrimp, similar to those reported by Howe (1987). The burrows may have originally been lined with bacteria that promoted methane oxidation and carbonate precipitation within the burrows. Variation in the material filling the burrows (e.g., siliciclastic sediments, calcitic spar, and cements) and the carbon isotopic composition of the infill indicate how long and how often the burrows acted as methane conduits. In the seep deposits from the Campanian Pierre Shale of Colorado, Krause et al. (2009) argued that the presence of meniscate and vesiculate fabrics attests to the former presence of bubbles. The

Fig. 15.21 Wood fall near AMNH loc. 3504, Custer County, South Dakota. A. Overview of the log (AMNH 135076). It is 2.8 m long and preserved inside a concretion. B. Close-up of a bivalve on the surface of the log. C, D. Cross sections through the black crusty outer layer of the log showing the thin white lenses of crushed shell debris. E, F. *Baculites compressus*, AMNH 161727, in the same concretion as the log, lateral and adapical views, respectively

bubbles would have entrained siliciclastic grains and at the same time promoted authigenic precipitation of carbonate, followed by precipitation of blocky calcite spar inside the tubes.

15.12.2 Water Depth

All the seeps in the US Western Interior, ranging from the Cenomanian to the early Maastrichtian, formed in relatively shallow water. The depth of the WIS during the deposition of the upper Campanian and lower Maastrichtian Pierre Shale was ≤100 m (Gill and Cobban 1966; Kauffman et al. 1996). This is consistent with interpretations based on foraminiferal assemblages (Bergstresser 1981; Howe 1987; Laird and Belanger 2018; Meehan et al. 2018). In addition, Kiel et al. (2012) cited the presence of cyanobacteria in concretions from the Cenomanian Tropic Shale of Utah as evidence that these seeps formed in the photic zone. In this respect, the seeps in the US Western Interior are similar to those in Spitsbergen, Svalbard, which also developed in an epicontinental sea setting (Hryniewicz et al. 2014).

15.12.3 Distance from the Shore

The seeps in the WIS formed in offshore settings, perhaps coincident with the forebulge depozone as suggested by Metz (2010) (however, see the earlier discussion on the origin of methane). According to reconstructions of the shoreline by Cobban et al. (1994), the seeps from the *Baculites scotti-Didymoceras nebrascense* Zones in Colorado formed 550 km east of the shoreline. The seeps of the same age in Wyoming, South Dakota, and Nebraska formed 225–325 km east of the shoreline (Cobban et al. 1994). The seeps from the *Baculites compressus* Zone in southwestern South Dakota developed 275 km east of the shoreline, although the position of the shoreline at that time is not well constrained (Landman and Klofak 2012).

Seeps may also have developed closer to shore, but no record of them exists. The higher permeability of coarser-grained sediments characteristic of nearshore sediments in the WIS would have facilitated the flow of methane but would not have promoted the development of a complex plumbing network. In addition, such sediments are typically organic poor and, thus, unlikely to have generated much methane by methanotrophic bacteria. Indeed, no seep deposits are known in the *Baculites compressus-B. reesidei* Zones of the Pierre Shale near Kremmling, Colorado, which represents a setting nearer the paleo-shoreline (Izett et al. 1971; Cobban et al. 1992).

15.12.4 Seeps as Refuges

Seeps may have represented semipermanent, self-sustaining habitats in the WIS even in times of environmental catastrophe. For example, volcanic ashfalls occasionally blanketed the WIS leading to widespread extermination of benthic and nektic fauna (Landman et al. 2018a, b). However, at seep sites, life may have persisted uninterruptedly because the local ecosystem was unimpaired (Brophy et al. 2018, 2022). Similarly, episodes of sea floor anoxia may have wrought havoc on broad swatches of the basin. However, if the seep deposits extended above the layer of low oxygenation, some animals may have survived (Landman et al. 2013). Larvae of these animals could then have repopulated other parts of the basin following the return of more hospitable conditions.

15.12.5 Expression of Seeps on the Sea Floor

In their study of the seep deposits from the *Baculites scotti-Didymoceras nebrascense* Zones of the Pierre Shale in Colorado, Kauffman et al. (1996) envisioned the seeps as having formed elevated carbonate chimneys up to 5 m above the sea floor, resulting from the concentrated movement of methane along a single channel. The chimney interfingered with the muddy sediments as it grew, reflecting starts and stops in methane emission. Kauffman et al. (1996) interpreted the concentric zonation of fossil assemblages around a central core as reflecting "a strong environmental gradient from chemically restrictive conditions around methane vents, across elevated, more-oxygenated mound flanks, and onto the dysoxic sea floor." They argued that the breakage of shells and their distribution on the flanks may have been due to slumping from higher slopes surrounding the central chimney. Kauffman et al. (1996) and Howe (1987) also identified slump blocks in the surrounding shale that were disjunct with the shale and suggested that these blocks fell down the slopes of the seep deposit onto the sea floor at the time the seeps were active.

The hypothesis of a chimney-like structure is complicated by the fact that the formation of seep carbonate involves AOM, which requires anoxic conditions and typically proceeds in the sulfate-methane transition zone 10s to perhaps 100s of centimeters below the sediment-water interface (Cochran et al. this volume). Formation of a chimney-like structure by AOM above the sediment-water interface requires anoxic conditions in the water column, as observed today, for example, on the northwestern shelf of the Black Sea and on the Nile deep-sea fan in the Mediterranean (Michaelis et al. 2002; Bayon et al. 2013). However, if the carbonate chimneys envisioned by Kauffman et al. (1996) developed in an anoxic water column, the faunal community associated with the chimneys would not have survived.

Carbonate chimneys can develop in an oxic water column under special circumstances. For example, Teichert et al. (2005) observed carbonate chimneys 10s of meters high at Hydrate Ridge on the Cascadia margin off the coast of Oregon. They

hypothesized that formation of these chimneys was due to mats of sulfide-oxidizing bacteria (*Beggiatoa*) that effectively coated the carbonate and provided an interface between the oxic water column and the underlying anoxic environment containing the archaean-bacterial consortium in which AOM and carbonate formation occurs. The formation of chimneys, as envisioned by Kauffman et al. (1996), would have required a similar, microbially mediated scenario.

In contrast, we argue that the seeps in the WIS did not form chimneys on the sea floor but were expressed instead as features with little or no relief. Authigenic precipitation of carbonate occurred below the sediment-water interface in the sulfate-methane transition zone. Seep deposits with an abundance of irregular, platy SACs would have appeared as crusts on the sea floor (Fig. 15.22). These crusts were periodically exhumed by bottom currents, exposing the hard rocky substrate (see Kiel (2010) for a description of modern seeps with a similar appearance, for example, in the Gulf of Mexico). This is consistent with the presence of organisms such as sponges, crinoids, and bryozoa that required a hard surface for attachment.

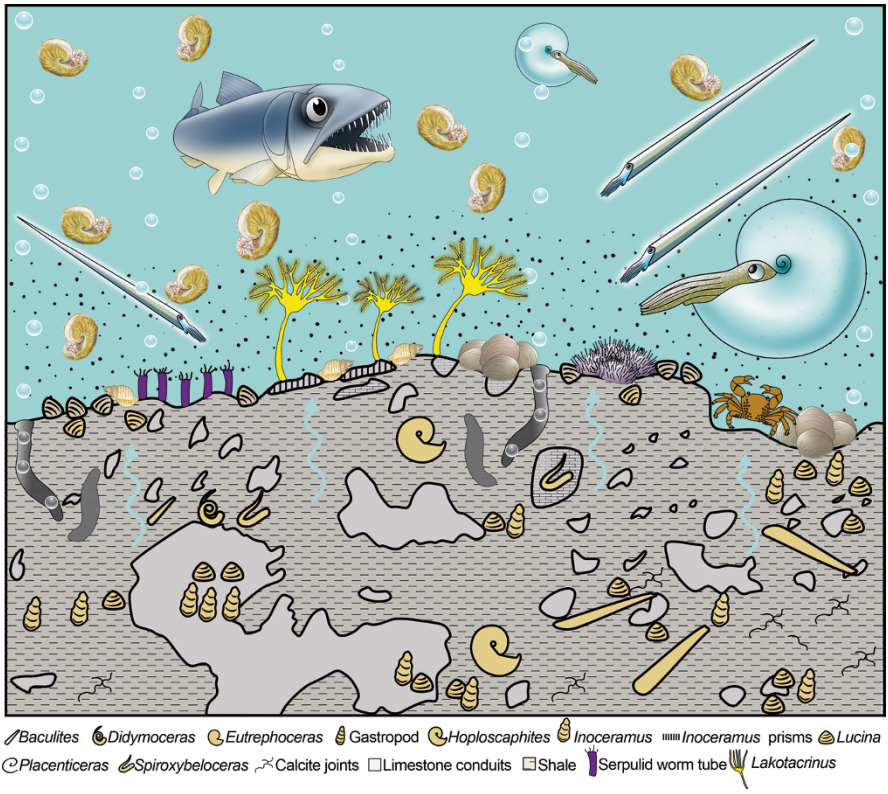

Fig. 15.22 Hypothetical reconstruction in cross section of a methane seep deposit in South Dakota during the late Campanian. The ammonites are species of *Hoploscaphites*, *Didymoceras*, *Spiroxybeloceras*, *Baculites*, and *Placenticeras*. (Reprinted from Landman et al. (2018a, b), used by permission of the *American Journal of Science*)

Colonization by inoceramids and oysters would have further stabilized this substrate, producing a platy, tabular pavement.

Seep deposits with large masses of vuggy, peloidal limestone containing numerous articulated lucinids would also have appeared as limestone crusts on the sea floor. The rapid authigenic precipitation of carbonate would have preserved the infauna living in the sediment (e.g., lucinids) as well as the epifauna living on the surface (e.g., inoceramids) and the nekton that settled to the bottom (e.g., ammonites, fish, mosasaurs). Differences in the abundance and size of vugs in the limestone are probably related to variation in the rate of flow and concentration of methane. The bubbles would have fragmented the authigenic deposits producing fractures and micritic clasts. Such brecciation and corrosion may have permitted occasional flushing of the bottom with more oxygen-rich waters. The broken-up micritic clasts were rapidly cemented together by syndepositional lithification, which probably occurred at the same rate as sediment aggradation.

Seep deposits that feature large, massive, micritic carbonates surrounded by shale containing subspherical SACs and pipes would not have been expressed on the sea floor except for the emission of seep fluids into the overlying water column (see Cochran et al. this volume). Advective transport of methane along fractures and preexisting burrow systems likely resulted in the formation of the large limestone masses at or below the sediment-water interface. Diffusion of methane in the sediments led to the formation of the subspherical SACs, which occasionally preserved organisms inside them (Figs. 15.12, 15.13 and 15.14). The presence of horizontal lenses of crushed inoceramid shells in some of these deposits indicates that these seeps occasionally developed accumulations of shelly debris on the sea floor. However, these accumulations were not extensive enough to attract animals that required hard substrates such as crinoids, sponges, and bryozoa.

15.13 Conclusions

Seep deposits in the Upper Cretaceous Western Interior of North America appear today as prominent geomorphic features in the landscape. They vary in shape depending on the size and lithology of the carbonate bodies that make up the deposits. They are geographically widespread; the bulk of them range from the upper middle Campanian to the early Maastrichtian, lasting for a duration of approximately 7 Myr. The presence of methane has been confirmed by isotopic analyses of the seep carbonates, which exhibit values of $\delta^{13}C$ as low as −50‰ VPDB. These low values of $\delta^{13}C$ indicate that the carbon was derived from bacterially mediated methane oxidation, thereby increasing the concentration of dissolved inorganic carbon and promoting the authigenic precipitation of carbonate minerals. The likely source of the methane was biogenic, produced by the decomposition of sedimentary organic matter, originating from the Pierre Shale and underlying formations.

Differences in the structure, lithofacies, and fossil composition of seep deposits may reflect differences in the duration and rate of methane emission. It is possible that the vugginess and low number of SACs (seep-associated concretions) observed

in deposits from the *Baculites scotti-Didymoceras nebrascense* Zones of the Pierre Shale in Colorado are due to high concentrations of methane emerging as bubbles into the overlying water via a central conduit. As a result, these deposits may have appeared as low-relief features on the sea floor. In contrast, the seep deposits from the *D. cheyennense-B. compressus* Zones of the Pierre Shale in South Dakota with massive, micritic carbonates and abundant SACs in the surrounding shale probably formed via diffuse methane flow at or below the sediment-water interface in the sulfate-methane transition zone. In some of these deposits, authigenic precipitation of carbonates resulted in the development of hard, irregular limestone crusts that were periodically exhumed by sediment dispersal.

Seeps formed unique habitats on the sea floor of the WIS in an otherwise homogenous environment. The most striking feature of these seeps is the abundance of organisms relative to the paucity in the surrounding shale. Most seep species reflect the background fauna of the WIS and are not seep-obligate. In general, the fauna is abundant but not diverse, with only a few species being dominant. Because all of these seeps developed at nearly the same water depth, any variation in faunal abundance among them is not due to variation in water depth but rather to variation in the chemical gradients on the sea floor and in the overlying water column reflecting the persistence and rate of methane flow and the concentrations of dissolved oxygen and hydrogen sulfide. Low values of $\delta^{13}C$ and elevated values of $^{87}Sr/^{86}Sr$ in the shells of well-preserved ammonites collected at seeps suggest that the chemistry of the overlying water column was affected by the seep fluids.

One of the most important factors controlling faunal abundance and diversity at the seeps was the nature of the substrate, consisting of either soft clayey mud or hard carbonate crusts. The development of hard crusts provided suitable substrates for animals to settle on and attach to, allowing for the formation of unique communities. These communities included stalked articulate crinoids, feather stars, sponges, ophiuroids, asteroids, regular and irregular echinoids, tube worms, crabs, bryozoa, and corals. In turn, these communities attracted a diverse suite of other organisms including gastropods, scaphites, baculites, nautilids, fish, and mosasaurs.

Acknowledgments At the American Museum of Natural History, we thank Ana Rashkova, Bushra Hussaini, Mary Conway, Kathleen Sarg, and Marion Savas for accessioning material and assigning AMNH numbers, Mariah Slovacek and Ana Raskhova for collecting fossils in the field and preparing specimens, and Stephen Thurston for photographing specimens and preparing figures. We thank Barbara A. Beasley for arranging permits to collect on the Buffalo Gap National Grassland, South Dakota. We thank Cheryl L. Metz for calling our attention to the maps of the Black Hills produced by N. H. Darton. Many students, colleagues, and family members have helped us collect in the field and interpret the results, and we wish to express our thanks to the ranchers, farmers, and private landowners who granted us permission to collect on their property: Malcolm Bedell, Gale Bishop, Shannon Brophy, Jim and Joyce Grier, William Halligan, Kayla Irizarry, Steve Jorgensen, the late Susan Klofak, Ekaterina Larina, Luke Larson, Tom Linn, Jone Naujokaityte, Dustin Perriguey, Remy Rovelli, James Witts, Adiel Klompmaker, Joshua Slattery, Joshua Laird, Christina Robins, Ben Thuy, Aaron Hunter, Tatsuo Oji, Paul Taylor, Ted Hubbard, Daniel Blake, Mary Haas, Andrzek Kaim, George Philips, Robert Jenkins, and all the doctors who treated us after our field injuries. This research was supported, in part, by the N.D. Newell Fund (AMNH). We are grateful for incisive reviews by William Halligan, Stephen Kiel, Russell Shapiro, and Andrzej Kaim whose comments substantially improved this manuscript.

Appendix

Table 15.1 AMNH localities, Pierre Shale. Abbreviations: *B. bac.*, *Baculites baculus*; *B. comp.*, *Baculites compressus*; *B. cun.*, *Baculites cuneatus*; *B. scotti*, *Baculites scotti*; *D. chey.*, *Didymoceras cheyennense*; *D. neb.*, *Didymoceras nebrascense.* Study number is a waypoint number (WPT) assigned by J. Brezina

Loc.	Study no. (WPT)	Zone	State	County	TRS	Latitude (N)	Longitude (W)
3342	–	*B. scotti-D. neb.*	SD	Fall River	SW 1/4 SEC 2, T8S, R7E	43° 22′ 48″	103° 15′ 19″
3344	–	*B. scotti-D. neb.*	SD	Butte	SE 1/4 SEC 9, T9N, R7E	44° 45′ 20″	103° 16′ 29″
3386	–	*B. scotti-D. neb.*	SD	Butte	NW 1/4 SEC 17, T9N, R7E	44° 44′ 47″	103° 17′ 47″
3418	59	*D. chey.*	SD	Custer	SEC 14, T3S, R10E	43° 47′ 18″	102° 53′ 20″
3419	61	*B. comp.*	SD	Custer	SEC 30 T3S, R11E	43° 45′ 41″	102° 51′ 9″
3420	61	*D. chey.*	SD	Custer	SEC 19, T3S, R11E	43° 46′ 15″	102° 51′ 26″
3440	36	*B. scotti-D. neb.*	SD	Butte	NW 1/4 SEC 10, T10N, R6E	44° 50′ 23″	103° 22′ 33″
3456	75	*B. comp.*	SD	Pennington	SEC5, T4S, R11E	43° 44′ 8″	102° 49′ 30″
3489	90	*D. chey.*	SD	Pennington	W 1/2 SEC 35, T3S, R12E	43° 45′ 11″	102° 39′ 36″
3494	–	*D. neb.*	WY	Weston	SE 1/4 SEC 18, T43N, R61W	43° 42′ 3″	104° 13′ 55″
3504	98	*B. comp.*	SD	Custer	SEC 19, T4S, R10E	43° 41′ 36″	102° 58′ 36″
3507	60	*B. comp*.	SD	Pennington	SEC 14, T2S, R10E	43° 52′ 42”	102° 53′ 30”
3509	130A, B	*D. chey.*	SD	Pennington	SEC 15, T2S, R10E	43° 52′ 39″	102° 54′ 40″
3528	174	*B. comp.-B. cun.*	SD	Meade	SEC 35, T3N, R14E	44° 10′ 22″	102° 24′ 6″
3529	140	*D. chey.*	SD	Pennington	SEC 3, T2S, R10E	43° 54′ 22″	102° 54′ 27″
3545	63	*B. comp.-B. cun.*	SD	Meade	SEC 18, T4N, R15E	44° 18′ 35″	102° 21′ 2″
3654	136	*D. chey.*	SD	Custer	SEC10, T5S, R9E	43° 37′ 50″	103° 2′ 26′
3666/3531	150	*B. scotti*	NB	Sioux	SEC 19, T34N, R55W	42° 54′ 54″	103° 51′ 19″

(continued)

Table 15.1 (continued)

Loc.	Study no. (WPT)	Zone	State	County	TRS	Latitude (N)	Longitude (W)
3686	67	*B. comp.*	SD	Custer	–	43° 53′ 33”	102° 43′ 41”
3812	79	*D. chey-B. comp.*	SD	Dawson	SEC2, T2S, R11E	43° 54′ 11″	102° 45′ 34″
3911	173	*B. bac.*	MT	Dawson	SEC15, T13N, R56E	46° 52′ 48″	104° 37′ 17″
–	69	*B. jenseni*	MT	Musselshell	–	47° 47′ 34”	107° 48′ 26”

References

Anderson J, Shapiro R, Lyons T (2005) Petrology and petrography of the Tepee Buttes (Cretaceous) methane-deep carbonates. In: Abstracts with programs, Geological Society of America 37:138

Arthur MA, Kauffman EG, Scholle PA et al (1982) Chemical and paleobiological evidence for the submarine spring origin of carbonate mounds in the Pierre Shale (Cretaceous of Colorado). In: Abstracts with programs, Geological Society of America 14:435

Barron EJ (1983) A warm, equable Cretaceous: the nature of the problem. Earth Sci Rev 19:305–338

Bash E, Shapiro R, Anderson J et al (2005) Distribution and mapping of the Cretaceous Tepee Buttes of the Western Interior Seaway. In: Abstracts with programs, Geological Society of America 37:138

Bayon G, Dupré S, Ponzevera E et al (2013) Formation of carbonate chimneys in the Mediterranean Sea linked to deep-water oxygen depletion. Nat Geosci 6:755–760

Bergstresser TJ (1981) Foraminiferal biostratigraphy and paleobathymetry of the Pierre Shale, Colorado, Kansas, and Wyoming. University of Wyoming, Dissertation

Birgel D, Peckman J, Klautzch S et al (2006) Anaerobic and aerobic oxidation of methane at Late Cretaceous seeps in the Western Interior Seaway, USA. Geomicrobiol J 23:565–577

Bishop GA, Williams AB (2000) Fossil crabs from tepee buttes, submarine seeps of the Late Cretaceous Pierre Shale, South Dakota and Colorado, USA. J Crustac Biol 20(2):286–300

Blake DB, Halligan WK, Larson NL (2018) A new species of the asteroid (Echinodermata) genus *Betelgeusia* from methane seep settings, Late Cretaceous of South Dakota. J Paleontol 92(2):196–206

Blakey R (2014) Paleogeography of the Western Interior Seaway of North America. Western Interior Seaway (NAM) series. Late Campanian (*B. compressus*). Used by permission: Colorado Plateau Geosystems https://deeptimemaps.com/map-room/. Accessed 21 Nov 2021

Boetius A, Ravenschlag K, Schubert CJ et al (2000) A marine microbial consortium apparently mediating anaerobic oxidation of methane. Nature 407:623–626

Brezina JA, Larson NL, Landman NH (2019) Fossil wood fall and associated fauna from the Late Cretaceous Western Interior Seaway in South Dakota. Paper presented at second international workshop on ancient hydrocarbon seep and cognate communities, Sapporo, Hokkaido, Japan, 13–15 June 2019

Brophy SK, Garb MP, Landman NH et al (2018) Biotic response to a Late Cretaceous ash fall: comparative faunal analyses from a methane seep and non-seep ecosystem within the Western Interior Seaway. Abstracts with programs, Geological Society of America 50(6):257–214

Brophy SK, Garb MP, Naujokaityte J et al (2022) Methane seeps as possible refugia during ash falls in the Late Cretaceous Western Interior Seaway. Geology 50(4):442–447

Cobban WA, Jeletzky JA (1965) A new scaphite from the Campanian rocks of the Western Interior of North America. J Paleontol 39(5):794–801

Cobban WA, Reeside JB Jr (1952) Correlation of the Cretaceous formations of the Western Interior of the United States. Geol Soc Am Bull 63:1011–1044

Cobban WA, Kennedy WJ, Scott GR (1992) Upper Cretaceous heteromorph ammonites from the *Baculites compressus* Zone of the Pierre Shale in north-central Colorado. US Geol Surv Bull 2024:A1–A11

Cobban WA, Mereweather EA, Fouch TD et al (1994) Some Cretaceous shorelines in the Western Interior of the United States. In: Caputo MV, Peterson JA, Franczyk KJ (eds) Mesozoic systems of the Rocky Mountain region, USA. Rocky Mountain Section Society for Sedimentary Geology, Denver, Colorado, pp 393–413

Cobban WA, Walaszczyk I, Obradovich JD et al (2006) A USGS zonal table for the Upper Cretaceous Middle Cenomanian-Maastrichtian of the Western Interior of the United States based on ammonites, inoceramids, and radiometric ages. US Geol Surv Open-File Rep 2006-1250:1–46

Cochran JK, Landman NH, Turekian KK et al (2003) Paleoceanography of the Late Cretaceous (Maastrichtian) Western Interior Seaway of North America: evidence from Sr and O isotopes. Palaeogeog Palaeoclimat Palaeoecol 191:45–64

Cochran JK, Kallenberg K, Landman NH et al (2010) Effect of diagenesis on the Sr, O, and C isotope composition of Late Cretaceous mollusks from the Western Interior Seaway of North America. Am J Sci 310:69–88

Cochran JK, Landman NH, Larson NL et al (2015) Geochemical evidence (C and Sr isotopes) for methane seeps as ammonite habitats in the Late Cretaceous (Campanian) Western Interior Seaway. Swiss J Paleontol 134(2):153–165

Cochran, JK, Landman NH, Jakubowicz M et al (this volume) Chapter 1: Geochemistry of cold hydrocarbon seeps: an overview. In: Kaim A, Cochran JK, Landman NH (eds) Ancient hydrocarbon seeps. Topics in Geobiology, vol. 50. Springer, Cham

Collom CJ, Johnston PA (2000) Late Cretaceous seep facies in the Western Interior of Canada and the United States: iron ooids, carbonate mounds, and associated tectonism. In: Program with extended abstracts (CD), GeoCanada 2000 Millenium Geoscience Summit, University of Calgary, Alberta, 29 May–2 June 2000

Corbett MJ, Watkins DK (2013) Calcareous nannofossil paleoecology of the mid-Cretaceous Western Interior Seaway and evidence of oligotrophic surface waters during OAE2. Palaeogeog Palaeoclimat Palaeoecol 392:510–523

Covey C, Sloan LC, Hoffert MI (1996) Paleoclimate data constraints on climate sensitivity: the paleocalibration method. Clim Chang 32:165–184

Cross TA (1986) Tectonic controls of foreland basin subsidence and Laramide style deformation, western United States. In: Allen PA, Homewood P (eds) Foreland basins. International Association of Sedimentology Special Publications, vol 8, Blackwell Scientific, Oxford, pp 15–39

Dahl RM, Close HG, Parsons-Hubbard K et al (2005) Paleoecology and topographic expression of a Cretaceous cold-seep: a taphonomic analysis of the Tepee Butte limestone. In: Abstracts with programs, Geological Society of America 37(7):138

Dane CH, Pierce WG, Reeside JB Jr (1937) The stratigraphy of the Upper Cretaceous rocks north of the Arkansas River in eastern Colorado. US Geol Surv Prof Pap 186-K:207–232

Darton NH (1902) Oelrichs folio: South Dakota–Nebraska. United States Geologic Survey Geologic Atlas of the United States 85. United States Geological Survey, Reston, Virginia

Darton NH (1904) Newcastle folio: Wyoming–South Dakota. United States Geological Survey Geologic Atlas of the United States 107. United States Geological Survey, Reston, Virginia

Darton NH (1905) Preliminary report on the geology and underground water resources of the central Great Plains. US Geol Surv Prof Pap 32:1–108

Darton NH (1919) Newell folio: South Dakota. United States Geological Survey Geologic Atlas of the United States 209. United States Geological Survey, Reston, Virginia

Darton NH, O'Harra CC (1909) Belle Fourche folio: South Dakota. United States Geological Survey Geologic Atlas of the United States 164. United States Geological Survey, Reston, Virginia

Darton NH, Paige S (1925) Central Black Hills folio: South Dakota. United States Geological Survey Geologic Atlas of the United States 219. United States Geological Survey, Reston, Virginia

Dennis KJ, Cochran JK, Landman NH et al (2013) The climate of the Late Cretaceous: new insights from the application of the carbonate clumped isotope thermometer to Western Interior Seaway macrofossils. Earth Planet Sci Lett 362:51–65

Elias MK (1931) The geology of Wallace County, Kansas. Kansas Geol Surv Bull 18:1–254

Elias MK (1933) Cephalopods of the Pierre Formation of Wallace County, Kansas, and adjacent area. Univ Kansas Sci Bull 21(9):289–363

Fenneman NM (1931) Physiography of western United States. McGraw-Hill, New York

Finlay GJ (1916) Colorado Springs folio: Colorado. United States Geological Survey Geologic Atlas of the United States 203. United States Geological Survey, Reston, Virginia

Fisher CA (1906) Nepesta folio: Colorado. United States Geological Survey Geologic Atlas of the United States 135. United States Geological Survey, Reston, Virginia

Fisher CG, Arthur MA (2002) Water mass characteristics in the Cenomanian Western Interior Seaway as indicated by stable isotopes of calcareous organisms. Palaeogeog Palaeoclimat Palaeoecol 188:189–213

Fricke HC, Foreman BZ, Sewall JO (2010) Integrated climate model-oxygen isotope evidence for a North American monsoon during the Late Cretaceous. Earth Planet Sci Lett 289:11–21

Gilbert GK (1896) The underground water of the Arkansas Valley in eastern Colorado. US Geol Surv Ann Rept 17(2):551–601

Gilbert GK (1897) Pueblo folio: Colorado. United States Geological Survey Geologic Atlas of the United States 36. United States Geologic Survey, Reston, Virginia

Gilbert GK, Gulliver FR (1895) Tepee buttes. Geol Soc Am Bull 6:333–342

Gill JR, Cobban WA (1966) The Red Bird section of the Upper Cretaceous Pierre Shale in Wyoming. US Geol Surv Prof Pap 393-A:1–73

Hall J, Meek FB (1856) Description of new species of fossils, from the Cretaceous formations of Nebraska, with observations upon *Baculites ovatus* and *B. compressus*, and the progressive development of the septa in *Baculites*, *Ammonites*, and *Scaphites*. Mem Am Acad Arts Sci 5:379–411

Hay WW (2008) Evolving ideas about the Cretaceous climate and ocean circulation. Cret Res 29:725–753

He S, Kyser TK, Caldwell WGE (2005) Paleoenvironment of the Western Interior Seaway inferred from $\delta^{18}O$ and $\delta^{13}C$ values of molluscs from the Cretaceous Bearpaw marine cyclothem. Palaeogeog Palaeoclim Palaeoecol 217:67–85

Howe B (1987) Tepee Buttes: a petrological, paleontological, paleoenvironmental study of Cretaceous submarine spring deposits. Thesis, University of Colorado

Howe B, Kauffman EG (1986) Tepee Buttes, late Campanian submarine springs and the biofacies, between Colorado Springs and Boone, Colorado. In: Kauffman EG (ed), Cretaceous biofacies of the central part of the Western Interior Seaway: a field guidebook. 4th North American Paleontological Convention, University of Colorado, Boulder, pp 155–175

Hryniewicz K (this volume) Appendix: Fossil seeps of the world. In: Kaim A, Cochran JK, Landman NH (eds) Ancient hydrocarbon seeps. Topics in Geobiology, vol 50. Springer, Cham. (Appendix)

Huber BT, Norris RD, MacLeod KG (2002) Deep-sea paleotemperature record of extreme warmth during the Cretaceous. Geology 30:123–126

Hudson JD, Anderson TF (1989) Ocean temperatures and isotopic compositions through time. Earth Environ Sci Trans R Soc Edinburgh: Earth Sci 80(3/4):183–192

Hunter AW, Larson NL, Landman NH et al (2016) A new crinoid from cold methane seep deposits in the Upper Cretaceous Pierre Shale. J Paleontol 90(3):506–524

Hunter AW, Brezina J, Larson NL (2018) Comment to Kato et al. (2017), Paleoecology of echinoderms in cold seep environments revealed by isotope analysis in the Late Cretaceous Western Interior Seaway. PALAIOS 33(6):282–283

Hyatt A (1903) Pseudoceratites of the Cretaceous. US Geol Surv Monogr 44:1–351

Izett GA, Cobban WA, Gill JR (1971) The Pierre Shale near Kremmling, Colorado, and its correlation to the east and the west. US Geol Surv Prof Pap 684-A:1–19

Jenkyns HC, Forster A, Schouten S et al (2004) High temperatures in the Late Cretaceous Arctic Ocean. Nature 432:888–892

Kato M, Oji T, Shirai K (2017) Paleoecology of echinoderms in cold seep environments revealed by isotope analysis in the Late Cretaceous Western Interior Seaway. PALAIOS 32:218–230

Kato M, Oji T, Shirai K (2018) Reply to comment on Kato et al. (2017) Paleoecology of echinoderms in cold seep environments revealed by isotope analysis in the Late Cretaceous Western Interior Seaway. PALAIOS 33(6):284–285

Kauffman EG (1984) Paleobiogeography and evolutionary response dynamic in the Cretaceous Western Interior Seaway of North America. In: Westermann GEG (ed), Jurassic–Cretaceous biochronology and paleogeography of North America. Geol Ass Canada Spec Pap 27:273–306

Kauffman EG, Caldwell WGE (1993) The Western Interior Basin in space and time. In: Caldwell WGE, Kauffman EG (eds), Evolution of the Western Interior Basin. Geol Ass Can Spec Pap 39:1–30

Kauffman EG, Arthur MA, Scholle P et al (1990) Lithofacies, biofacies, and geochemistry of the Tepee Buttes, Late Campanian (Cretaceous) submarine springs, Pueblo-Boone area, southern Colorado: Cretaceous rhythms, events and resources field trip. University of Colorado, Boulder

Kauffman EG, Arthur MA, Howe B et al (1996) Widespread venting of methane-rich fluids in Late Cretaceous (Campanian) submarine springs (Tepee Buttes), Western Interior Seaway, U.S.A. Geology 24:799–802

Kiel S (ed) (2010) The vent and seep biota: aspects from microbes to ecosystems. Topics in Geobiology, vol 33. Springer, Cham

Kiel S, Weise F, Titus AL (2012) Shallow-water methane-seep faunas in the Cenomanian Western Interior Seaway: no evidence for onshore-offshore adaptations to deep-sea vents. Geology 40(9):839–842

Krause FF, Clark J, Sayegh SG et al (2009) Tube worm fossils or relic methane expulsing conduits? PALAIOS 24:41–50

Kruta I, Landman NH, Rouget I et al (2011) The role of ammonites in the Mesozoic marine food web revealed by jaw preservation. Science 331:70–72

Laird JD, Belanger CL (2018) Quantifying successional change and ecological similarity among Cretaceous and modern cold-seep faunas. Paleobiology 45(1):114–135

Landman NH, Klofak SM (2012) Anatomy of a concretion: life, death, and burial in the Western Interior Seaway. PALAIOS 27:672–693

Landman NH, Kennedy WJ, Cobban WA et al (2010) Scaphites of the '*nodosus* group' from the Upper Cretaceous (Campanian) of the Western Interior of North America. Bull Am Mus Natl Hist 342:1–242

Landman NH, Cochran JK, Larson NL et al (2012) Methane seeps as ammonite habitats in the U.S. Western Interior Seaway revealed by isotopic analyses of well-preserved shell material. Geology 40(6):507–510

Landman NH, Kennedy WJ, Cobban WA et al (2013) A new species of *Hoploscaphites* (Ammonoidea: Ancyloceratina) from cold methane seeps in the Upper Cretaceous of the U.S. Western Interior. Am Mus Novit 3881:1–39

Landman NH, Grier JC, Grier JW et al (2015) 3-D orientation and distribution of ammonites in a concretion from the Upper Cretaceous Pierre Shale of Montana. Swiss J Paleontol 134(2):257–279

Landman NH, Cochran JK, Slovacek M et al (2018a) Isotope sclerochronology of ammonites (*Baculites compressus*) from methane seep and non-seep sites in the Late Cretaceous

Western Interior Seaway, USA: implications for ammonite habitat and mode of life. Am J Sci 318:603–639

Landman NH, Jicha BR, Cochran JK et al (2018b) $^{40}Ar/^{39}Ar$ date of a bentonite associated with a methane seep deposit in the upper Campanian *Baculites compressus* Zone, Pierre Shale, South Dakota. Cret Res 90:90–96

Landman NH, Kennedy WJ, Larson NL et al (2019) Description of two species of *Hoploscaphites* (Ammonoidea: Ancyloceratina) from the Upper Cretaceous (lower Maastrichtian) of the U.S. Western Interior. Bull Am Mus Natl Hist 427:1–72

Landman NH, Kennedy WJ, Grier J et al (2020) Large scaphitid ammonites (*Hoploscaphites*) from the Upper Cretaceous (upper Campanian–lower Maastrichtian) of North America: endless variation on a single theme. Bull Am Mus Natl Hist 441:1–131

Larson NL, Jorgensen SD, Farrar RA et al (1997) Ammonites and the other cephalopods of the Pierre Seaway. Geoscience Press, Tucson, Arizona

Larson NL, Brezina J, Landman NH et al (2014) Hydrocarbon seeps: unique habitats that preserved the diversity of fauna in the Late Cretaceous Western Interior Seaway. Wyoming Geological Society Guidebook, Caspar, Wyoming. https://www.academia.edu/4641897/Hydrocarbon_seeps_unique_habitats. Accessed 4 Nov 2021

Lavington CS (1933) Montana Group in eastern Colorado. Am Assoc Pet Geol Bull 17:397–410

Lukeneder A, Harzhauser M, Müllegger S et al (2010) Ontogeny and habitat change in Mesozoic cephalopods revealed by stable isotopes ($\delta^{18}O$, $\delta^{13}C$). Earth Planet Sci Lett 296:103–114

Lynds RM, Slattery JS (2017) Correlation of the Upper Cretaceous stratigraphy of Wyoming. Wyoming State Geol Surv Open File Rept:2017–2013

Mapel WJ, Pillmore CL (1963) Geology of the Newcastle area, Weston County, Wyoming. US Geol Surv Bull 1141-N:1–85

Meehan K, Landman NH (2016) Faunal associations in cold-methane seep deposits from the Upper Cretaceous Pierre Shale, South Dakota. Palaios 31(6):291–301

Meehan KC, Mego Vela M, Gilles NV et al (2018) Foraminifera from the upper Campanian Pierre Shale methane cold-seeps. South Dakota Cret Res. https://doi.org/10.1016/j.cretres.2018.03.023

Meek FB (1876) A report on the invertebrate Cretaceous and Tertiary fossils of the upper Missouri country. US Geol Surv Terr Rept 9:1–629, pls 1–45

Meek FB, Hayden FV (1856) Descriptions of new species of Gasteropoda from the Cretaceous formations of Nebraska Territory. Proc Acad Natl Sci Phila 8:63–69

Merewether EA, McKinney KC (2015) Chronostratigraphic cross section of Cretaceous formations in western Montana, western Wyoming, eastern Utah, northeastern Arizona, and northwestern New Mexico, U.S.A. US Geol Surv Open-File Rept 2015–1087. https://doi.org/10.3133/ofr20151087

Metz CL (2002) Upper Cretaceous (Campanian) sequence and biostratigraphy, west Texas to east-central Utah and development of cold-seep mounds in the Western Interior Cretaceous basin. Texas A&M University, Dissertation

Metz CL (2010) Tectonic controls on the genesis and distribution of Late Cretaceous, Western Interior Basin hydrocarbon seep mounds (tepee buttes) of North America. J Geol 118:201–213

Michaelis W, Seifert R, Nauhaus K et al (2002) Microbial reefs in the Black Sea fueled by anaerobic oxidation of methane. Science 297:1013–1015

Morton SG (1834) Synopsis of the organic remains of the Cretaceous group of the United States illustrated by nineteen plates, to which is added an Appendix containing a tabular view of the Tertiary fossils hitherto discovered in North America. Biddle, Philadelphia

Morton SG (1842) Description of some new species of organic remains of the Cretaceous group of the United States: with a tabular view of the fossils hitherto discovered in this formation. J Acad Natl Sci Phila 8(2):207–227

Owen DD (1852) Report of a geological survey of Wisconsin, Iowa, and Minnesota; and incidentally of a portion of Nebraska Territory made under instructions from the United States Treasury Department, 2 vols. Lippincott, Grambo, Philadelphia

Petta TJ, Gerhard LC (1977) Marine grass banks, a possible explanation for carbonate lenses, Tepee Zone, Pierre Shale (Cretaceous), Colorado. J Sediment Res 47(3):1018–1026
Robinson CS, Mapel WJ, Cobban WA (1959) Pierre Shale along western and northern flanks of Black Hills, Wyoming and Montana. Am Ass Pet Geol Bull 43:101–123
Robinson CS, Mapel WJ, Bergendahl MH (1964) Stratigraphy and structure of the northern and western flanks of the Black Hills Uplift, Wyoming, Montana, and South Dakota. US Geol Surv Prof Pap 404:1–134
Rowe A, Landman NH, Witts JW et al (2020) Late Cretaceous methane seeps as habitats for newly hatched ammonites. PALAIOS 35:1–13
Ryan D, Witts JD, Landman NH (2020) Paleoecological analysis of a methane seep in the Late Cretaceous (Maastrichtian) Western Interior, USA. Lethaia 54:185–203
Sahling H, Galkin SV, Salyuk A et al (2003) Depth-related structure and ecological significance of cold-seep communities—a case study from the Sea of Okhotsk. Deep-Sea Res Part I 50:1391–1409
Say T (1820) Observations on some species of zoophytes, shells, &c. principally fossil. Am J Sci Arts 2(2):34–45
Schröder-Adams C (2014) The Cretaceous Polar and Western Interior seas: paleoenvironmental history and paleoceanographic linkages. Sediment Geol 301:26–40
Scott GR (1969) General and engineering geology of the northern part of Pueblo, Colorado. US Geol Surv Bull 1262:1–131
Scott GR, Cobban WA (1965) Geologic and biostratigraphic map of the Pierre Shale between Jarre Creek and Loveland. Colorado US Geol Surv Misc Geol Invest Map Ser I-439. scale 1:48,000
Scott GR, Cobban WA (1975) Geology and biostratigraphic map of the Pierre Shale in the Canon City-Florence Basin and the Twelvemile Park area, south-central Colorado. US Geol Surv Misc Geol Invest Map Ser I-937. scale 1:48,000
Scott GR, Cobban WA (1986a) Geologic and biostratigraphic map of the Pierre Shale in the Colorado Springs-Pueblo area. Colorado. US Geol Surv Misc Geol Invest Map Ser I-1627. scale 1:100,000
Scott GR, Cobban WA (1986b) Geology, biostratigraphic, and structure map of the Pierre Shale between Loveland and Round Butte. Colorado. US Geol Surv Misc Geol Invest Map Ser I-1700. scale 1:50,000
Shackleton NJ, Kennett JP (1975) Paleotemperature history of the Cenozoic and initiation of Antarctic glaciation: oxygen and carbon isotope analyses in DSDP sites 277, 279 and 281. Init Rep Deep Sea Drilling Prog 29:743–755
Shapiro RS (2004) Recognition of fossil prokaryotes in Cretaceous methane seep carbonates: relevance to astrobiology. Astrobiology 4:438–449
Shapiro RS, Fricke H (2002) Tepee buttes: fossilized methane-seep ecosystems. In: Leonard EM et al (eds), High Plains to Rio Grande Rift: Late Cenozoic evolution of central Colorado. Geol Soc Am Field Guide 3:94–101
Shapiro RS, Gale CM (2001) Bacterial fossils from Cretaceous methane-seep carbonates. In: Abstracts with programs, Geological Society of America 33(6):A453
Sharps JA (1976) Geologic map of the Lamar Quadrangle. Colorado and Kansas US Geol Surv Misc Geol Invest Map Ser I-944. scale 1:250,000
Sharps JA (1980) Geologic map of the Limon 1″ X 2″ quadrangle, Colorado and Kansas. US Geol Surv Misc Geol Invest Map Ser I-1250., scale 1:250,000
Spicer RA, Corfield RM (1992) A review of terrestrial and marine climates in the Cretaceous with implications for modeling the 'Greenhouse Earth.' Geol Mag 129:169–180
Stephenson LW (1941) The larger invertebrates of the Navarro Group of Texas (exclusive of corals and crustaceans and exclusive of the fauna of the Escondido Formation). Univ Texas Bull 4101:1–641
Teichert BMA, Bohrmann G, Suess E (2005) Chemoherms on Hydrate Ridge—unique microbially-mediated carbonate build-ups growing into the water column. Palaeogeog Palaeoclimat Palaeoecol 227:67–85

Thuy B, Landman NH, Larson NL et al (2018) Brittle star mass occurrence on a Late Cretaceous methane seep from South Dakota, USA. Sci Rep 8-9617:1–9

Tobin TS, Ward PD (2015) Carbon isotope ($\delta^{13}C$) differences between Late Cretaceous ammonites and benthic mollusks from Antarctica. Palaeogeog Palaeoclimat Palaeoecol 428:50–57

Tsujita CJ, Westermann GEG (1998) Ammonoid habitats and habits in the Western Interior Seaway: a case study from the Upper Cretaceous Bearpaw Formation of southern Alberta, Canada. Palaeogeog Palaeoclimat Palaeoecol 144:135–160

Tweto O (1980) Summary of Laramide orogeny in Colorado. In: Kent HC, Porter KW (eds), Colorado geology. Proceedings, Symposium on Colorado geology, Denver, pp 129–134

Weise F, Kiel S, Pack A et al (2015) The beast burrowed, the fluid followed—crustacean burrows as methane conduits. Mar Pet Geol 66(3):631–640

Whitfield RP (1877) Preliminary report on the paleontology of the Black Hills, containing descriptions of new species of fossils from the Potsdam, Jurassic, and Cretaceous formations of the Black Hills of Dakota. US Geographical and Geological Survey of the Rocky Mountain Region, Washington, DC

Wright EK (1987) Stratification and paleocirculation of the Late Cretaceous Western Interior Seaway of North America. Geol Soc Am Bull 99:480–490